Pergamon

Bioorganic & Medicinal Chemistry, Vol. 4, No. 11, pp 1881–1899, 1996

PII: S0968-0896(96)00171-X
0968-0896/96 $15.00+0.00

Glycopeptide Mimics of Mammalian $Man_9GlcNAc_2$. Ligand Binding to Mannan-binding Proteins (MBPs)

Henrik Franzyk,[a] Morten Meldal,*[,a] Hans Paulsen,[b] Steffen Thiel,[c] Jens Chr. Jensenius[c] and Klaus Bock[a]

[a]*Department of Chemistry, Carlsberg Laboratory, Gamle Carlsberg Vej 10, DK-2500 Valby, Copenhagen , Denmark*
[b]*Institute of Organic Chemistry, University of Hamburg, Martin-Luther-King-Platz 6, D-20146 Hamburg, Germany*
[c]*Department of Medical Microbiology and Immunology, University of Aarhus, Universitetsparken, DK-8000 Århus C, Denmark*

Abstract—A novel and simple approach for rational design of oligosaccharide mimics has been developed. Mammalian high-mannose triantennary structure $Man_9GlcNAc_2$ has been subjected to molecular modelling using the NMR data available on structural fragments of the oligosaccharide. The analysis indicated four different low energy conformations, and the spatial arrangement of terminal disaccharides of the oligosaccharide antennae were simulated with glycopeptides carrying disaccharides by applying weak constraints between the saccharide parts in MD-simulations on a large array of tri- to octaglycopeptides. The five glycopeptides exhibiting the best fit with the four minimum energy conformations of the oligosaccharide were synthesized by solid phase glycopeptide assembly using glycosylated fluoren-9-ylmethyloxycarbonyl-amino acid-*O*-pentafluorophenyl esters as building blocks. The glycan was acyl protected α-D-Man-(1→2)-α-D-Man and Ser, Thr and Hyp were the glycosylated amino acids. The deprotected and purified glycopeptides were subjected to NMR analysis for characterization, and in order to investigate the *cis–trans* isomerism of the carbimide bonds to Hyp. The glycopeptides were tested for their ability to inhibit binding of mannan-binding protein to mannan from *Saccharomyces cerevisiae*. They were found to be weak inhibitors showing no indication of multivalent interaction with the mannan-binding protein. Copyright © 1996 Elsevier Science Ltd

Introduction

In recent years the interest in glycobiology has grown considerably, which may be attributed to the recognition of cell surface carbohydrates as cell–type specific markers which mediate cell-pathogen and cell–cell interactions (e.g. cell adhesion). An increasing number of these important biological processes exhibiting sugar-specificity have been shown to involve lectins capable of binding endogenous carbohydrate ligands as well as polysaccharides on bacteria, viruses and parasites.

Animal lectins can conveniently be divided into three major groups based on the amino acid sequence similarity of their carbohydrate-recognition domains[1] (CRDs) since their overall structure exhibits a high degree of diversity. These three lectin classes are usually designated P-type (e.g. the mannose-6-phosphate receptors), C-type (calcium ion-dependent), and S-type (soluble β-galactoside-binding).

Mannose 6-phosphate receptors are further subgrouped into the monomeric cation-independent (CI) receptors and the dimeric cation-dependent (CD) receptors. The CI receptor contains 15 CRDs of which only two domains appears to be involved in oligosaccharide binding, by contrast only one CRD motif is present in the CD receptor. Hence both receptors show high affinity for diphosphorylated oligosaccharide ligands.

The C-type lectins form a heterogenous class of proteins, which can be divided into several subgroups:[1] (i) endocytic receptors with type I transmembrane orientation, e.g. the mannose receptor of macrophages and hepatic endothelial cells; (ii) endocytic receptors with type II transmembrane orientation, e.g. the asialoglycoprotein receptor of hepatocytes, Kupffer cell receptor and chicken hepatic lectin; (iii) adhesion molecules, i.e. the selectins located on T cells and lymphocytes (L-type), on endothelium (E-type) and on platelets (P-type); (iv) proteoglycans; and (v) the collectins.

The collectins comprise a group of soluble, circulating proteins, of which the mannan-binding proteins (synonyms: mannose-binding proteins, MBPs), the pulmonary surfactant apoproteins (e.g. SP-A and SP-D), conglutinin and collectin-43 (CL-43) are the main members.[1,2] Mannan-binding proteins (MBPs) have been demonstrated in the serum of several mammalian species, e.g. humans,[3] cows,[4] rabbits,[5] rats[6] and mice,[7] and recently also in chicken.[8] In general, collectins form oligomeric bouquets or cruciform structures (except for the monomeric CL-43) of trimeric subunits each composed of three polypeptide chains coiled up in a collagenous triple-helical arrangement. Each polypeptide chain ends in a globular carbohydrate recognizing domain (CRD) with a single binding site for oligo- and polysaccharide structures with terminal Man, Glc, GlcNAc or L-Fuc residues. Recently, the crystal structure of human MBP[9] was

elucidated, and the distance between the carbohydrate binding sites in the trimeric subunits was found to be as long as ~45 Å. Thus, simultaneous ligation of such three CRDs appears to require a very large oligosaccharide or polysaccharide ligand. Alternatively, the possibility exists that several trimer heads, either within an oligomer or from different bouquets, are capable of binding smaller oligosaccharides.

The stalk region of the collectins resembles closely that of the C1q-protein (C1q) in the complement cascade. In fact, C1q and MBP share a similar overall structure which also gives rise to a similarity in their host defence mechanisms:[10,11] while the globular heads of C1q binds multivalently to the Fc regions of antibodies clustered on antigen-containing pathogens, the MBP interacts multivalently with the polysaccharide of the pathogen. The C1r–C1s serine protease complex and MASP (MBP-associated serine protease) bind to the respective collagenous stalks and then activate the classical complement pathway.[12–14] Moreover, MBP has complement-dependent bactericidal activity.[15] In addition, direct interaction[10] of the collagen part of MBP-pathogen complexes with cell surface receptors may trigger oxidative killing or phagocytosis, e.g. complement-independent opsonization[16] of *Salmonella montevideo*. Low levels of MBP in a subgroup of the population are associated with recurrent infections, especially in infants,[17] also supporting that MBPs might be part of a primitive innate immune system.

Interestingly, high-mannose oligosaccharide-containing glycopeptides may be involved in the physiological regulation of immunocompetent cells as previously demonstrated by in vitro assays.[18] The observed biological activities included stimulation of interleukin 1(IL-1) synthesis, induction of prostaglandin (PGE_2) production, and the induction of a delayed-type inflammatory response following intradermal injection. Such potent N-linked oligosaccharides were obtained from ovalbumin and soybean agglutinin, and they consisted of penta-, hexa- and nonamannosides linked to asparagine via two GlcNAc residues. Among these three types of compounds, the glycopeptide $Man_9GlcNAc_2$-Asn exhibited the diverse range of biological activities, listed above, in addition to inhibition of antigen driven T cell proliferation.[18] However, the mechanism by which these high-mannose oligosaccharides elicit their biological activities remains to be elucidated.

A previous study[19] showed that the yeast analogues of such high-mannose structures may be involved in the defense system of plants. Attack by pathogenic microorganisms is usually met with an active defence response of the plant, which includes (i) induction of enzymes of secondary metabolism, e.g. phenylalanine ammonia-lyase (PAL), (ii) modification of cell walls, (iii) induction of lytic enzymes, and (iv) production of the plant hormone ethylene.[19]

Small peptides carrying N-linked high-mannose structures were found to act as elicitors on nM scale in this defence response of tomato cells.[19] These elicitors were prepared by α-chymotrypsin cleavage of yeast invertase, and therefore they deviate structurally from the animal type of high-mannoses (see Scheme 1 for an example).

For a given peptide backbone, the highest elicitor activity was seen when 10–12 mannosyl residues were present in the glycan moiety (i.e. $Man_{10-12}GlcNAc_2$) while glycopeptides Asn-N-linked to $Man_9GlcNAc_2$ and $Man_8GlcNAc_2$ (yeast type) exhibited 3- and 100-fold lower activity, respectively. Furthermore, the results indicated that the elicitor activity is almost independent of the structure of the peptide backbone. However, positively charged amino acids (e.g. Arg and His) seem to enhance the potency while the hydrophobic amino acid Phe reduces it. Thus, a glycopeptide with the dipeptide backbone Arg-Asn still gave full defence response.[19] Interestingly, the high-mannose oligosaccharides, prepared by endoglycosidase H treatment of the above glycopeptides, were potent inhibitors of the ethylene stimulation in tomato plants.

Peptide scaffolds and framework have been widely used in the construction of synthetic molecular receptors and others devices.[20] The nature of peptides offers several advantages when designing complex structures (e.g. enzyme or receptor mimics). Natural amino acids are commercially available in chiral form and a large number of other amino acids have been prepared enantioselectively to ensure sufficient diversity of the available building blocks. Also, most important, versatile procedures for synthesis and purification are well established, and for small peptides characterization by NMR is feasible.

In particular, the special case of glycopeptides has been exploited to some extent. Thus, small glycopeptide

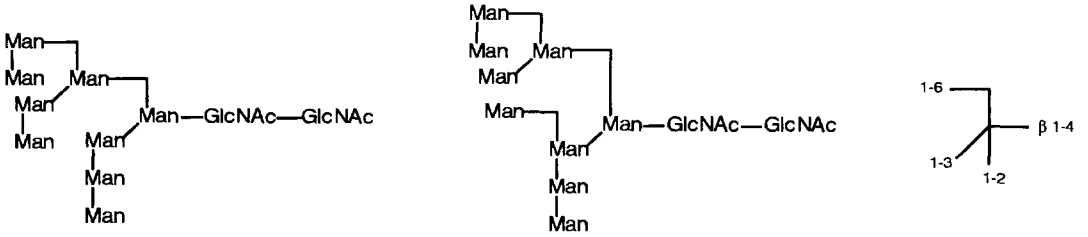

$Man_9GlcNAc_2$ structure found in mammals. $Man_9GlcNAc_2$ structure isolated from yeast.

Scheme 1. Differences in mammal and yeast high-mannose structures. Glycopeptides **5**, **7**, **9**, **11** and **13** were synthesized as mimics of the mammalian structure.

models of the hormone somatostatin have been reported[21] as tools for the examination of the putative enhancement of biological stability imposed on peptides upon glycosylation. More recently, this was further investigated[22] by GlcNAc-substitution of several major histocompatibility complex (MHC)-binding peptides, and the results showed marked stability against proteolytic degradation even when the glycosylation was rather distant from the cleavage site. Another example involves the synthesis of phytoalexin elicitor peptides[23] with β-D-Glc(1→6)α-D-Man(1→6)-D-Man *O*-linked to a serine residue. In addition, the introduction of a serine β-O-linked glucose moiety in analogues of enkephalin facilitated their transport across the blood–brain barrier without decreasing their ability to bind to the opioid receptors.[24] Sialophorin, a major surface glycoprotein of human leucocytes and platelets, contains mucin-type oligosaccharides possibly mediating independent T cell activation, and a partial glycopeptidic structure with a β-D-Gal(1→3)-α-D-GalNAc-Thr residue has recently been synthesized.[25]

Due to the variety of putative biological functions of high-mannose oligosaccharide structures, listed above, we were intrigued to design and synthesize glycopeptide mimics corresponding to several conformations of $Man_9GlcNAc_2$ (mammalian type: see Scheme 1). By this approach, the aim was to obtain a mimic of the biologically active conformation of the native oligosaccharide, which might be expected to show comparable or even considerably higher affinity than the oligosaccharide itself depending upon the abundance of the active conformation.

Here, a simple modelling procedure based on earlier molecular dynamic simulations and NMR data is presented. Previously, we have reported[26] on the synthesis of the *O*-dimannosyl amino acid building blocks **1–3**, which are N^{α}-fluoren-9-ylmethoxycarbonyl (Fmoc) protected pentafluorophenyl (Pfp) active esters. As they carry acyl protected α(1→2)-linked mannobiosides they were suitable for synthesis of glycopeptide mimics of mammalian $Man_9GlcNAc_2$ where the $Man_3GlcNAc_2$ core are replaced by a linear peptide template. Multiple-column peptide synthesis[27] (MCPS) as well as glycopeptide synthesis by the syringe method[28] were employed in the present work, since both methods have yielded satisfactory results[29,30] with similar small glycopeptide ligands for the mannose 6-phosphate receptor.

Results and discussion

Modelling of mammalian $Man_9GlcNAc_2$

As exemplified above, oligosaccharides of the high-mannose type appears frequently to be an essential part of bioactive compounds, and they may even be responsible for the biological function. Although the involved oligosaccharides may have a rather complex structure, often only the terminal monosaccharides or disaccharides actually interact with the corresponding receptor. Such examples include: (i) the hepatic asialoglycoprotein receptor, for which strongly interacting synthetic cluster ligands have been reported,[31–34] (ii) the mannose 6-phosphate receptor,[29,35] and (iii) the MBPs,[36,37] all of which have been studied with respect to the multivalency of ligand binding. Since the natural ligands for these receptors are not readily available in substantial amounts from natural sources or by synthesis,[38] it would be preferable to be able to prepare synthetic mimics of the complex oligosaccharides. Recently, we have reported on the successful synthesis of high-affinity ligands for the mannose 6-phosphate receptor[29]. These ligands were designed as glycopeptide templates conferring a similar spatial arrangement to the terminal mannose disaccharides as they have in the natural ligand.

In the present work, the mammalian $Man_9GlcNAc_2$ oligosaccharide was selected as a target for MD simulation and simple rational design of glycopeptide mimics.

First, the major conformations of mammalian $Man_9GlcNAc_2$ were considered from the previous NMR studies[39–41] of different oligomannosides and earlier MD simulations of such compounds[42] and of simple α(1→2)-, α(1→3)- and α(1→6)-linked mannose disaccharides.[43,44] Based on these reports and some initial minimizations on the mannose disaccharides using the InsightII/Discover package (from Biosym) with the Amber force field, the following values for the glycosidic bond torsional angles (see Scheme 2) in the initial conformations were employed: $(\phi, \psi) = (-45°, -20°)$ for the α(1→2)-linkages; $(\phi, \psi) = (-50°, -20°)$ for the α(1→3)-linkages, and $(\phi, \psi) = (-60°, 180°)$ for both the α(1→6)-linkages. For simplicity we adopted the ω angles (−60° and 60°) for the α(1→6)-linkages proposed by Rademacher et al.[41] to give rise to the four conformational populations upon NOE constrained AMBER minimization. The β(1→4) linkages between the core GlcNAcs and the first mannosyl residue were set to the initial values of $(\phi, \psi) = (55°, 0°)$ as found by Paulsen[45] and Meyer et al.[46] in other oligosaccharides featuring this moiety. In Figures 1 and 2, four such conformations are depicted

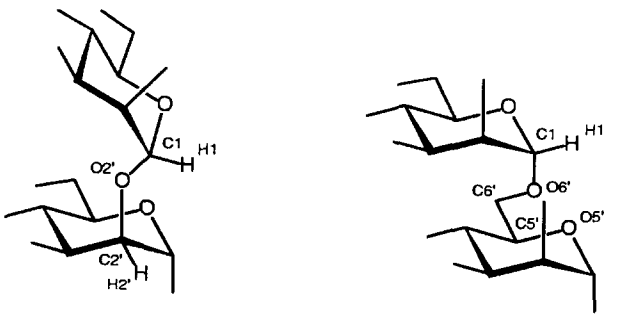

ϕ = H1-C1-O2'-C2'

ψ = C1-O2'-C2'-H2'

ϕ = H1-C1-O6'-C6'

ψ = C1-O6'-C6'-C5'

ω = O6'-C6'-C5'-O5'

Scheme 2. Definitions of the torsion angles ϕ, ψ, and ω.

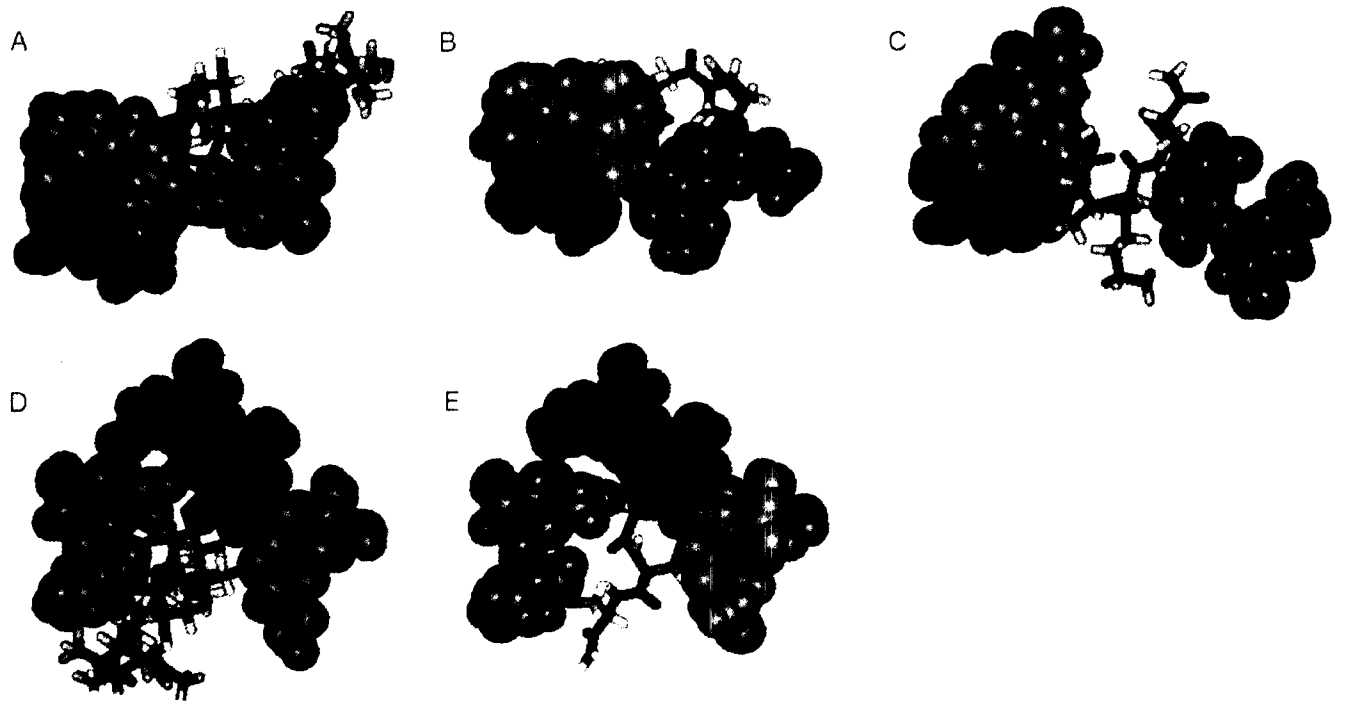

Figure 1. Comparison of extended mammalian $Man_9GlcNAc_2$ conformations with glycopeptide mimics. (A) Extended oligosaccharide conformation; (B and C) the corresponding glycopeptide mimic **5**, in the constrained model conformation and in the NMR based conformation, respectively; (D and E) extended oligosaccharide conformation and the corresponding glycopeptide mimic **9**, respectively.

(on the left-hand-sides); they were generated by minimization using the Discover/Amber force field at 300 K in vacuo. The steepest descend algorithm was used for the first 100 steps of energy minimization, whereas the conjugate minimization algorithm was used until the maximum derivative was below 0.05 kcal $Å^{-1}$. Most of the torsional angles in the minimized conformations deviated less than $\pm 10°$ from their

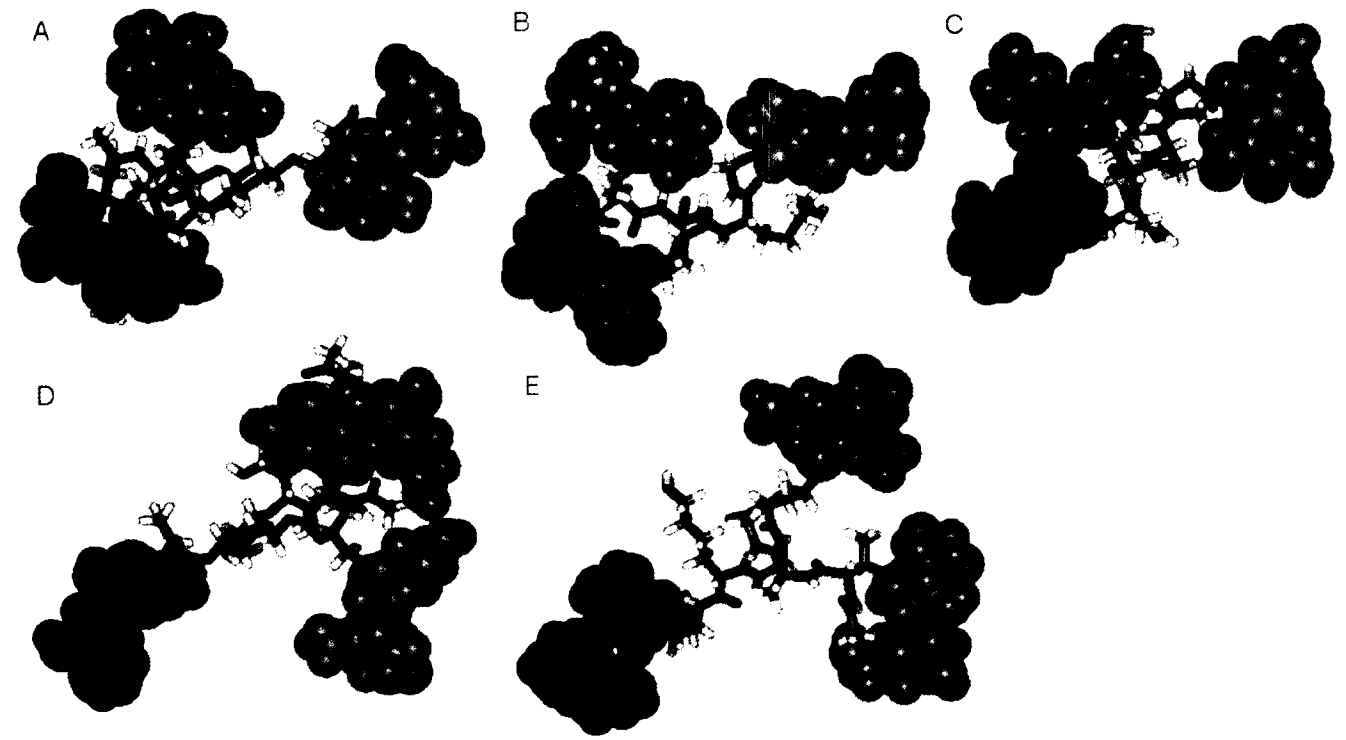

Figure 2. Comparison of backfolded mammalian $Man_9GlcNAc_2$ conformations with glycopeptide mimics. (A) Backfolded oligosaccharide conformation; (B and C) The corresponding glycopeptide mimic **11**, in the constrained model conformation and in the NMR based conformation, respectively. (D and E) Backfolded oligosaccharide conformation and the corresponding glycopeptide mimic **13**, respectively.

initial values. This and the fact that their relative total energy was in the range 2.5–5 kcal mol^{-1} strongly suggest that they are almost equally stable minimum energy conformations, of which only one might be responsible for the interaction with, e.g. MBP.

Selected distances between the three terminal Man(1→2)Man disaccharide moieties in the thus obtained four main low energy conformations were measured. Hence, the dimensions of the two triangles, formed by the O3s of the terminal mannose and of the inner C1s of the reducing mannose in these α(1→2)-linked dimannosyl units, were considered to be a sufficient requirement, which should be met by triglycosylated glycopeptide mimics. The scaffold of these four modelling targets were then replaced by a peptide backbone, containing Ser, Thr and/or Hyp glycosylation sites, in either of two ways: (i) the spatial arrangements of the terminal disaccharides of the four resulting models were maintained after removal of the core sugar residues, then amino acid residues were fitted manually until a satisfactory template was obtained, or (ii) a model of the peptide was build in the extended conformation, and subsequently three α(1→2)-linked mannobiosides were connected in their predominant conformation (ϕ, $\psi = -50°$, $-20°$). In order to situate all three sugars in the same direction X^1 was arbitrarily set to $-60°$, 60°, or 180°. When the distances between the disaccharide moieties of the model oligosaccharide conformation (e.g. in Figure 1C) were short, method (i) proved most convenient, otherwise method (ii) was employed, however, with both methods the calculations were performed as follows. During the dynamic simulation the selected target distances were typically constrained to within 1–2 Å (or even 0.5 Å when the distance criteria was reached easily, or 2.5 Å when the constraint proved difficult to satisfy) using an appropriate penalty force (5 kcal mol^{-1} $Å^{-2}$), which would allow that all carbohydrate residues maintained a chair conformation. Initially, a brief minimization (100 steps) of the potential glycopeptide mimics was performed. Subsequently, a constrained dynamic simulation (>10,000 steps of 1 fs) was run, and if no satisfactory fit to one of the desired oligosaccharide conformations could be obtained, the peptide template was discarded as a non-suitable candidate. Another sequence was then attempted (>50 in all). Finally, a constrained minimization of the selected MD-structures, which best fitted each of the structures of the $Man_9GlcNAc_2$, was performed. The resulting glycopeptide structures were compared by superposition with the parent oligosaccharide structure (see Figs 1 and 2), and for each of the four structural populations one to two synthetic targets were selected: Ac-Ser*-Ser*-Lys-Gly-Hyp*-NH_2 (**5**), Ac-Ser*-Gly-Thr*-Lys-Ser*-NH_2 (**7**)/Ac-Lys-Gly-Ser*-Ser*-Ser*-NH_2 (**9**), Ac-Thr*-Ala-Hyp*-Lys-Gly-Ser*-NH_2 (**11**) and Ac-Thr*-Ala-Gly-Hyp*-Gly-Lys-Ser*-NH_2 (**13**), where * denotes side chain glycosylation with α-D-Man(1→2)α-D-Man.

From the above modelling studies it was evident that the maximum distance (25–30 Å) between the terminal disaccharides in both the oligosaccharide and glycopeptide mimic would be less than the distance between the CRDs (45 Å) in a single trimeric subunit in human MBP. However, the clustering of trimers in the bouquet oligomers might enable multivalent binding of a single ligand due to the proximity of the sugar-binding site to the edge of each trimer, or more hypothetically this might allow binding to two different oligomers.

As is seen from the above list of synthetic target molecules, glycosylated hydroxyproline is present in three of the five compounds. This introduction of an unnatural glycosidic linkage was considered for several reasons. Previously, a large amount of the glycosylated Hyp building block had been prepared for use in libraries, however it was also examined as a new structural feature during the modelling studies. In fact, Hyp in the *trans* conformation proved valuable as a residue conferring rigidity to the glycopeptide as well as allowing the introduction of a distinct bend in the backbone, which seemed necessary for the models to present the disaccharide moieties appropriately. Furthermore, in this work the preferred non-glycosylated amino acids were Gly, Ala and Lys as they do not present any severe problems in solid phase synthesis. Furthermore, the side chain of lysine may be derivatized, e.g. with a fluorescent probe for biological evaluations, or may serve as a connecting arm to a secondary scaffold (e.g. a trivalent acid or a spacer peptide) allowing formation of even larger structures.

Synthesis of glycopeptide mimics

Glycopeptides **4**, **6**, **10** and **12** and reference peptides **14–17** (see Schemes 4–6) were synthesized simultaneously by MCPS[27] using dimethylformamide (DMF) as solvent and the PEGA resin (derivatized with the Rink-linker) as solid phase, whereas glycopeptide **8** was synthesized by the syringe method[28] under similar conditions.

The synthesis was performed with N^{α}-Fmoc protected amino acid Pfp esters with addition of 3,4-dihydro-3-hydroxy-4-oxo-1,2,3-benzotriazine (Dhbt-OH) as an auxiliary nucleophile; the *O*-dimannosyl units were introduced by application of the glycosylated building blocks **1–3** (see Scheme 3). Deprotection of Fmoc was achieved by treatment with 20% piperidine in DMF, and after the final deprotection the N-terminal was acetylated with 20% acetic anhydride in DMF. Cleavage from the linker was effected by treatment with 95% aqueous trifluoroacetic acid (TFA), and the crude (glyco)peptides were purified by preparative HPLC (in 16–69% yield, average ~50%). The sugar-protected glycopeptides were characterized by ^1H NMR (presented in Tables 1–4) and mass spectrometry (MALDI-TOF). In the assignments of ^1H NMR spectra, phase-sensitive COSY spectra readily afforded the amino acid chemical shifts and the intra-ring sugar correlations, whereas ROESY spectra were employed for the confirmation of the amino acid sequence (via H^{α}_n–$N^{\alpha}H_{n+1}$ correlations), and for obtaining inter-residue sugar connectivities (see Scheme 7).

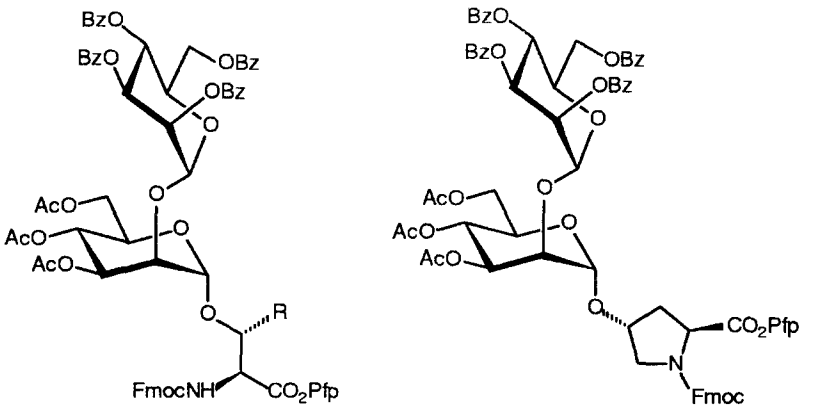

Scheme 3. Building blocks for solid-phase glycopeptide synthesis.

As it is seen from Tables 3 and 4, the chemical shifts of the sugar moieties of the protected glycopeptides are remarkably similar irrespective of the neighbouring amino acid residues, indicating the absence of interaction between the relatively polar backbone and the apolar acylated *O*-dimannosyl moieties.

Deacylation of the protected glycopeptides was performed with hydrazine hydrate[47] in chloroform–methanol[29] to ensure full solubility of both the starting material and the product. This procedure showed no indications of base-catalysed β-eliminations as side reactions. After an initial purification of the reaction mixture by gel permeation chromatography (to remove excess reagent and the co-product benzoyl hydrazide), final purification by HPLC gave pure unprotected glycopeptides **5**, **7**, **9**, **11** and **13** in moderate to high yields (51–96%; occurrence of the lower yield may possibly be ascribed to a too short reaction time and/or precipitation of educt).

Assignments of the ^{1}H NMR spectra of the deacylated glycopeptides was performed essentially as described for the sugar-protected glycopeptides, however, due to increased complexity of the carbohydrate region HMQC spectra were acquired to obtain reasonably narrow shift ranges for H-3, H-4, H-5 and H-6. The identity of the glycopeptides and reference peptides was confirmed by ES-MS.

The ^{1}H NMR chemical shifts of glycopeptides **5**, **7**, **9**, **11**, **13** and the corresponding non-glycosylated peptides **14–17** are presented in Tables 7 and 10: the shifts in δ-value (ppm) observed for the glycosylated position were very small (±0.1 for Ser, ±0.02 for Thr and ±0.01 ppm for Hyp) while the protons on the neighbouring carbons, consequently, were seen at slightly lower field (+0.15−0.2 ppm for Ser, +0.07−0.15 ppm for Thr, and +0−0.17 ppm for Hyp). Again, the chemical shifts (see Tables 8 and 9) of the sugar moieties in the glycopeptides were almost identical indicating the absence of interaction with the peptide backbone. Comparison with the ^{1}H NMR spectrum[48] (in D_2O) of native $Man_9GlcNAc_2$ shows that the terminal mannoses have similar chemical shifts (within ±0.05 ppm) while the H-1 and H-2 of the amino acid linked mannoses appears at slightly higher field (−0.3 to −0.1 ppm).

Furthermore, the Hyp and glycosyl-Hyp containing peptides appeared as *cis–trans* isomers in the NMR spectra (Tables 1, 2 and 5, 6) due to the rotational barrier of the carbimide bond between the Hyp amino group and the carboxyl group of the previous amino acid (see Scheme 8). The temperature dependence of this equilibrium was examined by recording ^{1}H NMR spectra at 278, 288, 300 and 313 K, but although quite large changes of the chemical shifts were observed no significant change in the isomer ratio was seen. Similar experiments on the building block **3** (in $CDCl_3$) were performed over the temperature range 253–313 K, and also in this case an almost constant *cis–trans* ratio of ~1:1 was found at all temperatures.

Next, the equilibrium was investigated by recording ^{1}H and ^{13}C NMR spectra, including ROESY and HMQC experiments, of peptides **14**, **16** and **17** in D_2O (see Tables 10 and 11).

From the ROESY spectra of **16** and **17** it was possible to determine the conformation of the major isomer as the NOEs indicated in Scheme 8 were present as well defined cross-peaks (see Fig. 3) except for the expected NOE of *cis*-**16** which was obscured by noise due to the vicinity of H^{γ}_{minor} to the HOD-signal. Thus, the major isomer of the Hyp-containing peptides has *trans* configuration. Furthermore, when comparing all the ^{1}H NMR spectra of Hyp-containing compounds it seems evident that the easily distinguishable β-protons of Hyp/glycosylated Hyp may be used for determining the *cis–trans* ratio, as the ^{1}H NMR signals of the *trans* isomer appear at higher field (0.1–0.2 ppm) than those of the *cis* isomer. In addition, the chemical shifts of the H^{γ}_{major} and H^{γ}_{minor} may be employed instead, as the

same distinct trend is seen for these sets of signals. The ^{13}C chemical shift differences between the two isomers (see Table 11) correspond closely to those reported[49] for the Gly-Hyp and Pro-Hyp dipeptides (also in D_2O),

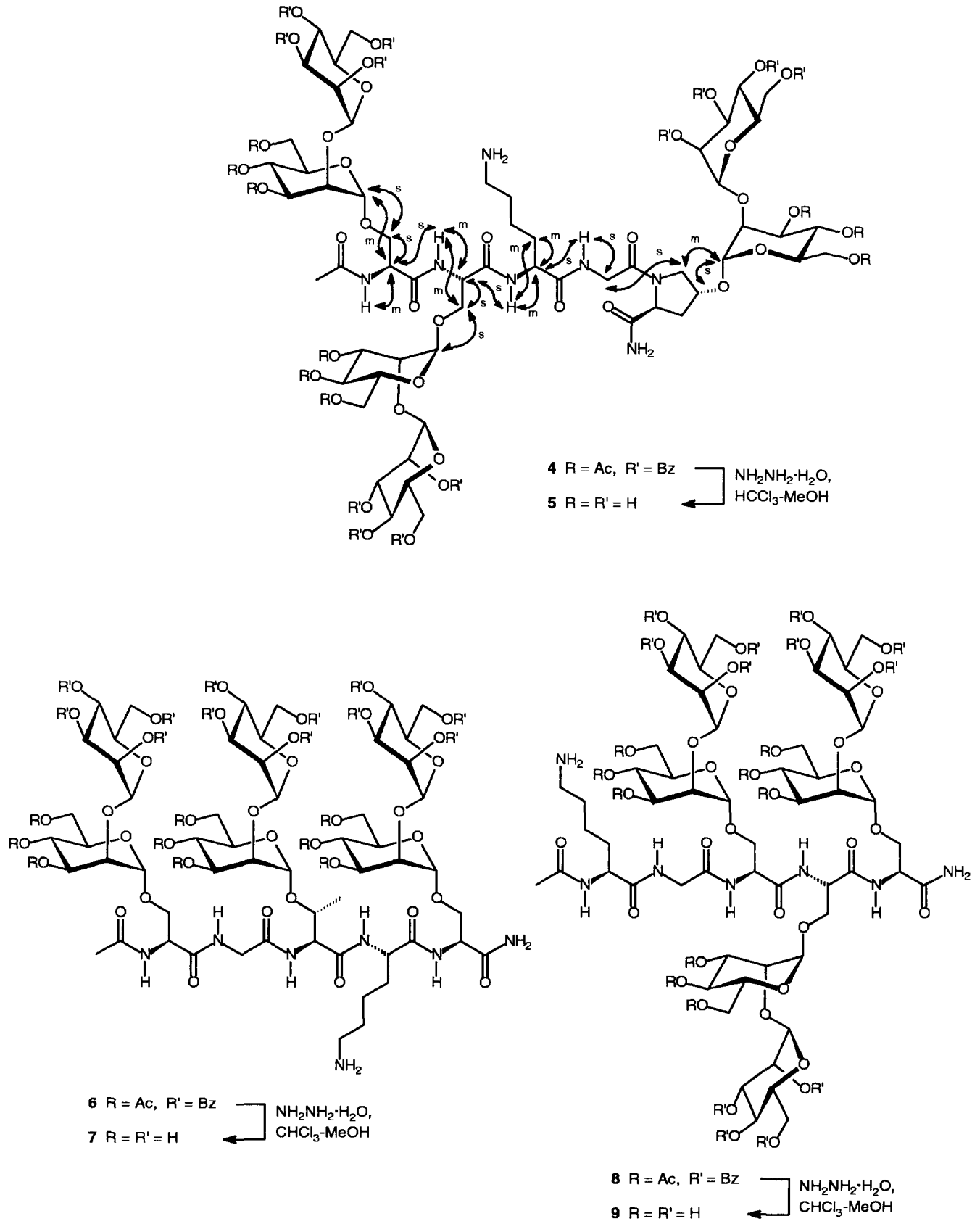

Scheme 4. Glycopeptidic mimics of extended conformations of mammalian $Man_9GlcNAc_2$. NOEs (strong: s and medium: m) for compound **5**.

which structures were confirmed by X-ray crystallographic studies. Based on these few examples of Hyp/glycosyl-Hyp containing peptides, a tendency towards decreasing abundance of the cis isomer is seen when the neighbouring amino acid residues become more bulky (e.g. terminal Hyp>-Gly-Hyp-Gly->-Ala-Hyp-Lys-). However, glycosylation seems only to have a very minor influence on the isomer ratio, at least for the present peptides.

Ligand binding studies

The binding affinity (IC_{50}) of glycopeptides **5**, **7**, **11** and **13** for human MBP was determined against yeast mannan from *Saccharomyces cerevisiae* in an ELISA type inhibition assay using the time resolved immunofluorometric assay (TRIFMA) technique. Microtitre wells coated with mannan were incubated with a mixture of MBP and a potential glycopeptidic inhibitor. Subsequent incubation with a monoclonal anti-MBP antibody labelled with europium allowed measurement of flurorescence on a time resolved spectrofluorometer.

In addition, a number of monosaccharides, methyl glycosides of monosaccharides, and 1,5-anhydropolyols, were tested as above, and the results of the ligand binding experiments are presented in Table 12. The activity was found to be low for all glycopeptides as might be expected from a previous investigation[37] of the MBP multivalency. The only simple ligands, which showed inhibition of mannan-binding was D-mannose, 1,5-anhydromannitol and methyl α-D-mannopyranoside, with the latter being most active indicating the α-glycosidic linkage to be important for the binding to MBP.

However, an acrylamide copolymer (molecular weight 1,500,000 to 2,000,000) having pendant chains of mammalian $Man_9GlcNAc_2$ has been reported very recently.[50] This $Man_9GlcNAc_2$-copolymer showed IC_{50} values in the μM scale when tested with recombinant rat mannose protein–carbohydrate recognizing domains (MBP-CRD) from serum. Thus, the long distance between the binding sites of the CRDs does not not allow simultaneous interaction neither with single trimers nor with several different trimers of the MBP oligomer, unless the ligand has a polymeric structure or at least is substantially larger than a single oligosaccharide unit.

The NOESY spectra of glycopeptides **5** and **11** were analysed with respect to the conformation of the backbone and sugar contacts. However, no assignable NOEs between different dimannosyl units were observed. In addition, the disaccharide moieties showed only NOEs to the peptide backbone at the site of attachment (see Schemes 4 and 5) also supporting conformations with the sugar residues pointing away

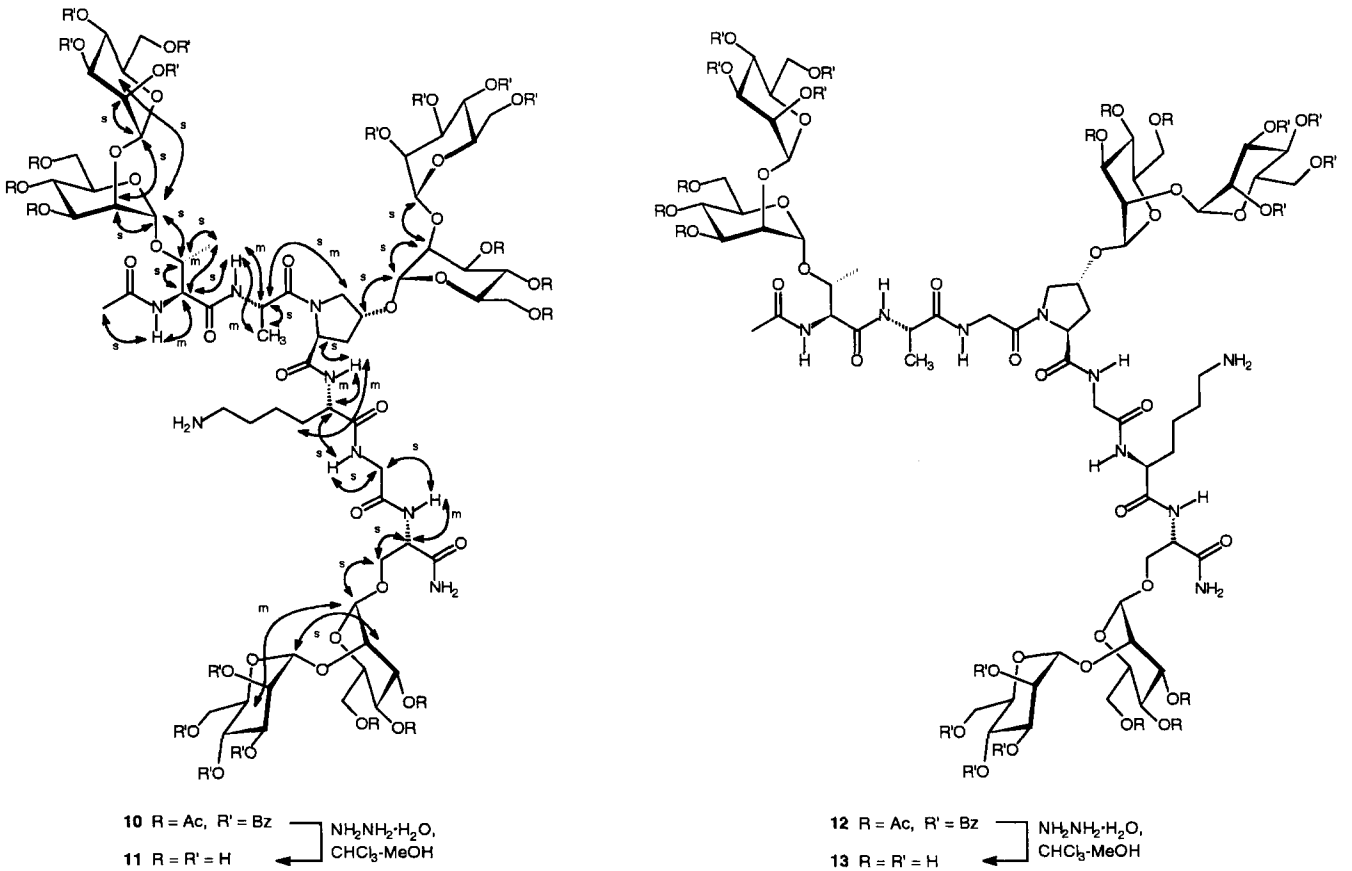

Scheme 5. Glycopeptidic mimics of extended conformations of mammalian $Man_9GlcNAc_2$. NOEs (strong: s and medium: m) for compound **11**.

from the core and each other. This assumption was confirmed by employing the obtained NOEs in a constrained MD calculation of compounds **5** and **11** where strong NOEs were set as distance constraints of 2–2.5 Å while medium strong NOEs were considered to correspond to distances of 2.5–3 Å (shown in Schemes 4 and 5). These MD calculations were performed as described above, and the results are depicted in Figures 1 and 2. A comparison (see Fig. 1) of the envisioned active conformation (B) of glycopeptide **5** and the conformation indicated from the NOEs (C) revealed that the conformational populations with all three the sugar units positioned rather closely apparently is less abundant in the solvent used (water–acetic acid-d_6, 1:1). Thus, NMR indicated only two of the disaccharides to be spatially close. This may results from a greater tendency to attain a more extended conformation of the backbone than observed in the original constrained model. For glycopeptide **11** (see Fig. 2) the deviation in distances between the distal 3- and 4-positions of the dimannosides in the $Man_9GlcNAc_2$-constrained model (B) and the NMR based model (C) were only 1–2 Å, however the orientation of the entire disaccharide moieties showed more severe differences.

Interestingly, the glycopeptide mimics of backfolded and extended structures, respectively, exhibited pairwise very similar behaviour on HPLC. Thus, glycopeptides **11** and **13** had identical retention times corresponding to a significantly lower polarity than that exhibited by the mimics of the backfolded structures (i.e. compounds **5**, **7** and **9**), which may reflect a similarity in overall shape.

In conclusion, a method of mimicking complex oligosaccharides with glycopeptides, starting from the preferred oligosaccharide conformations, was developed. Thus, the vast number of possible glycopeptide constructs was reduced by applying a constrained MD calculation based on the oligosaccharide structure. Only glycopeptides which were able to attain a considerable match with the predominant oligosaccharide conformations were selected as synthetic targets. The preferred conformation of the glycopeptide mimics according to NMR spectroscopy showed only limited resemblance to the conformations inferred by the initial MD calculations. However, such glycopeptide mimics having stable local energy minima in the desired conformations may well be able to adapt to the requirements of a putative receptor due to the high flexibility of the peptide backbone.[29] The biological evaluation of the $Man_9GlcNAc_2$ glycopeptide mimics as putative regulators of immunological processes[18] and as elicitors of a defence response[19] in plants are currently being performed.

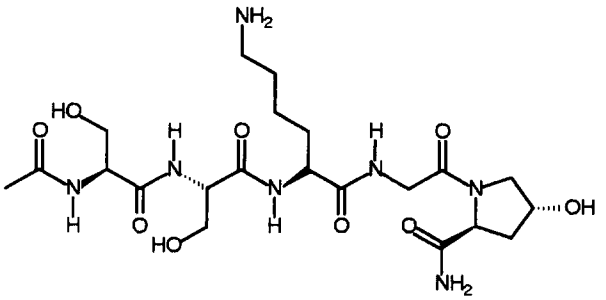

14

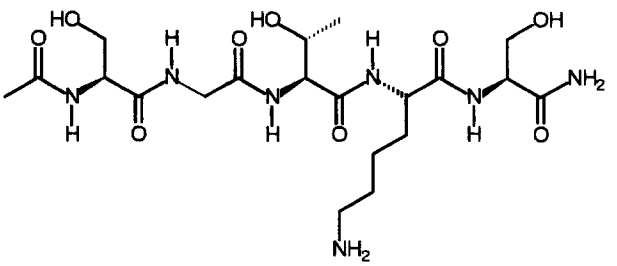

15

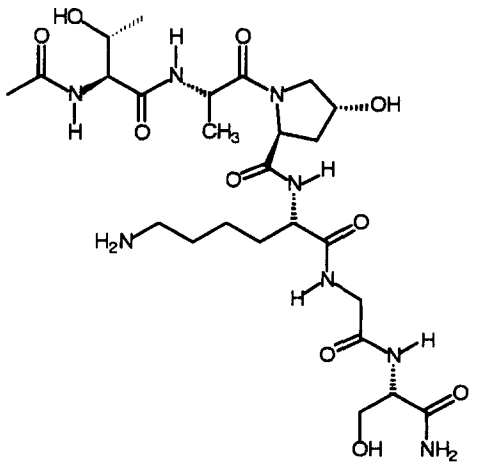

16

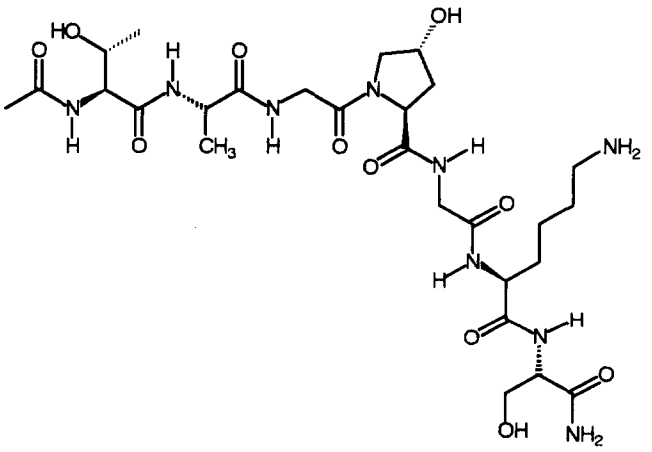

17

Scheme 6. Non-glycosylated reference peptides.

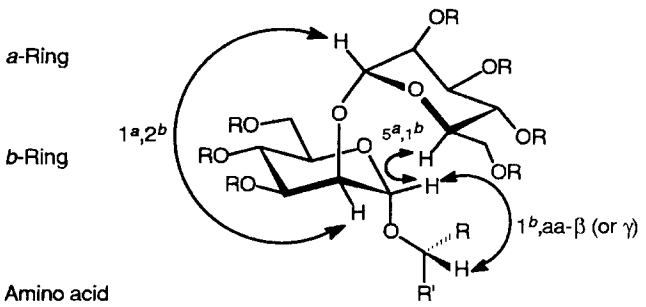

Scheme 7. Observed inter-ring NOEs for the *O*-dimannosyl moieties.

Experimental

General procedures

Dichloromethane was distilled from phosphorous pentoxide and kept over 3 Å molecular sieves. Pyridine was distilled and kept over 3 Å molecular sieves. Concentrations were performed under reduced pressure at temperatures <40 °C. Phosphorous oxychloride, 4-ethylmorpholine (NEM), 3,4-dihydro-3-hydroxy-4-oxo-1,2,3-benzotriazine (Dhbt-OH), hydrazine hydrate, and trifluoroacetic acid (TFA) were from Fluka. *O*-(1*H*-Benzotriazol-1-yl)-*N*,*N*,*N*′,*N*′-tetramethyluronium tetrafluoroborate (TBTU) was from

Table 1. ^{1}H NMR data (600 and 500 MHz, DMSO-d_6) for amino acids in sugar-protected glycopeptides **4**, **6** and **8**. Chemical shifts in ppm

	N$^\alpha$H	H$^\alpha$	H$^\beta$	H$^\gamma$	H$^\delta$	H$^\varepsilon$	AcHN
4							
Ser^a-1	8.32	4.67	3.92/3.64	—	—	—	1.89
Ser^a-2	8.44	4.63	3.92/3.69	—	—	—	—
Lys-3	8.09	4.37	1.71/1.54	1.35	1.52	2.75	—
Gly-4	8.02	4.01/3.83	—	—	—	—	—
Hyp^a-5	—	4.32	2.23/2.11	4.52	3.80/3.48	—	—
cis-5^b	—	4.48	—	—	—	—	—
6							
Ser^a-1	8.23	4.61	3.82/3.56	—	—	—	1.88
Gly-2	8.21	4.01/3.73	—	—	—	—	—
Thr^a-3	8.25	4.47	4.02	1.21	—	—	—
Lys-4	8.08	4.35	1.70/1.61	1.34	1.51	2.73	—
Ser^a-5	8.09	4.51	3.81/3.65	—	—	—	—
8							
Lys-1	7.99	4.19	1.63/1.47	1.29/1.24	1.46	2.71	1.89
Gly-2	8.10	3.79	—	—	—	—	—
Ser^a-3	8.31	4.74	3.95/3.68	—	—	—	—
Ser^a-4	8.44	4.73	3.91/3.73	—	—	—	—
Ser^a-5	8.40	4.54	3.84/3.68	—	—	—	—

^{a}Denotes side chain glycosylation with $Bz_4Man(1\rightarrow2)Ac_3Man$.
^{b} *Cis–trans* ratio of 15:85.

Table 2. ^{1}H NMR data (600 and 500 MHz, DMSO-d_6) for amino acids in sugar-protected glycopeptides **10** and **12**. Chemical shifts in ppm

	N$^\alpha$H	H$^\alpha$	H$^\beta$	H$^\gamma$	H$^\delta$	H$^\varepsilon$	AcHN
10							
Thr^a-1	8.16	4.44	4.05	1.07	—	—	1.88
Ala-2	8.01	4.59	1.17	—	—	—	—
Hyp^a-3^b	—	4.51	2.28/2.02	4.51	3.82/3.68	—	—
Lys-4	8.21	4.24	1.70/1.52	1.38	1.53	2.76	—
Gly-5	8.08	3.83/3.78	—	—	—	—	—
Ser^a-6	8.27	4.51	3.83/3.67	—	—	—	—
12							
Thr^a-1	8.24	4.40	4.02	1.17	—	—	1.92
Ala-2	8.09	4.35	1.22	—	—	—	—
Gly-3	7.99	4.04/3.81	—	—	—	—	—
Hyp^a-4	—	4.46	2.28/2.05	4.53	3.72/3.63	—	—
cis-4^c	—	4.63	—	—	—	—	—
Gly-5	8.41	3.79/3.68	—	—	—	—	—
Lys-6	7.96	4.33	1.69/1.57	1.32	1.52	2.75	—
Ser^a-7	8.22	4.52	3.86/3.68	—	—	—	—

^{a}Denotes side chain glycosylation with $Bz_4Man(1\rightarrow2)Ac_3Man$.
^{b}Less than 2% *cis*-isomer.
^{c}*Cis–trans* isomer ratio of 20:80.

Table 3. ^1H NMR data (600 and 500 MHz, DMSO-d_6) for sugar units in protected glycopeptides **4**, **6** and **8**. δ-Values in ppm

		1-H	2-H	3-H	4-H	5-H	6-H
4							
Ser-1	Man(1→2)	5.45[a]	5.68	5.81	6.05[b]	4.64	4.67/4.50
	Man(1→Ser)	5.23	4.23	5.25	5.33[a]	4.00	4.20/4.07[c]
Ser-2	Man(1→2)	5.44[a]	5.68	5.81	6.05[b]	4.64	4.67/4.50
	Man(1→Ser)	5.23	4.23	5.25	5.31[a]	4.00	4.19/4.01[c]
Hyp-5	Man(1→2)	5.45	5.68	5.81	6.05[b]	4.67	4.67/4.50
	Man(1→Hyp)	5.33	4.19	5.21	5.35	4.00	4.20/4.09[c]
6							
Ser-1	Man(1→2)	5.42	5.68	5.80[d]	6.04	4.61	4.66/4.47
	Man(1→Ser)	5.16[d]	4.16[d]	5.22[c]	5.30[c]	4.01[c]	4.20/4.01[c]
Thr-3	Man(1→2)	5.42	5.68	5.81[d]	6.06	4.66	4.76/4.49
	Man(1→Thr)	5.30	4.16	5.26	5.33	3.98	4.19/4.04
Ser-5	Man(1→2)	5.42	5.68	5.80[d]	6.05	4.63	4.66/4.49
	Man(1→Ser)	5.18[d]	4.18[d]	5.23[c]	5.31[c]	3.95[c]	4.17/4.04[c]
8							
Ser-3	Man(1→2)	5.43	5.68	5.79	6.05	4.63	4.67/4.48
	Man(1→Ser)	5.19	4.24[c]	5.26[c]	5.36[c]	4.03[c]	4.20/4.04
Ser-4	Man(1→2)	5.43	5.68	5.79	6.05	4.63	4.67/4.48
	Man(1→Ser)	5.24	4.25	5.25	5.34	4.04	4.20/4.04
Ser-5	Man(1→2)	5.43	5.68	5.79	6.05	4.63	4.67/4.48
	Man(1→Ser)	5.19	4.20[c]	5.25[c]	5.34[c]	3.99[c]	4.20/4.04

[a–d]Signals may be interchanged vertically in each column.
[b]Distinct very close signals (in each column).
[c]Horizontal sets of coupled signals, which may be vertically interchanged for each compound.

Bachem. The Rink-linker (4-[α(fluoren)-9-ylmethoxy-carbonylamino)-2,4-dimethoxybenzyl]phenoxy acetic acid) and suitably protected N^{α}-Fmoc amino acid Pfp esters were purchased from MilliGen (Taastrup, Denmark), NovaBiochem (Läufelfingen, Switzerland) or Bachem (Bubendorf, Switzerland). Electrospray mass spectrometry was performed in the positive mode for both peptides and deprotected glycopeptides on a Fisons VG Quattro Instrument. MALDI-TOF MS was performed in the positive mode for the protected glycopeptides on a Finnigan MAT 2000 using a matrix of α-cyano-4-hydroxycinnamic acid. ^1H and ^{13}C NMR spectra were recorded on a Bruker AM 500 MHz or an AMX 600 MHz spectrometer. Chemical shifts are given in ppm and referenced to external dioxane (δ_H 3.76, δ_C 67.40) for solutions in D_2O at 300 K. For spectra recorded in DMSO-d_6 and CD_3COOD-H_2O, the DMSO signal at 2.50 ppm and HOAc signal at 2.03 ppm, respectively, were used as internal references. For the assignment of signals, proton–proton (COSY) and HMQC shift correlation spectroscopy, and ROESY (rotational frame NOESY) and NOESY spectra were used. Preparative reverse phase HPLC separations were performed on a Waters HPLC system using a Delta PAK C-18 column (15 μm, 300 Å, 25 mm × 200 mm) with a flow rate of 10 mL min^{-1}, or a Delta PAK

Table 4. ^1H NMR data (600 and 500 MHz, DMSO-d_6) for sugar units in protected glycopeptides **10** and **12**. δ-Values in ppm

		1-H	2-H	3-H	4-H	5-H	6-H
10							
Thr-1	Man(1→2)	5.37	5.67	5.80[a]	6.10	4.61	4.80/4.45
	Man(1→Thr)	5.22	4.03	5.20	5.24	3.97	4.14/3.98
Hyp-3	Man(1→2)	5.44	5.68[a]	5.78[b]	6.07	4.66	4.72/4.49
	Man(1→Hyp)	5.30	4.19	5.20	5.31	3.98[a]	4.21/4.10[c]
Ser-6	Man(1→2)	5.49	5.68[a]	5.80[a,b]	6.05	4.64	4.67/4.51
	Man(1→Ser)	5.18	4.19	5.23	5.33	3.98[a]	4.19/4.05[c]
12							
Thr-1	Man(1→2)	5.41	5.68	5.80	6.07	4.62	4.73/4.49
	Man(1→Thr)	5.28	4.09	5.25	5.25	4.03	4.20/4.03
Hyp-4	Man(1→2)	5.46	5.68	5.80	6.04	4.66	4.68/4.51
	Man(1→Hyp)	5.31	4.22	5.23	5.36[c]	3.97[c]	4.19/4.06[c]
Ser-7	Man(1→2)	5.45	5.68	5.80	6.06	4.65	4.68/4.51
	Man(1→Ser)	5.21	4.21	5.23	5.30[c]	4.00[c]	4.21/4.10[c]

[a]Distinct very close signals (in each column).
[b]Signals may be vertically interchanged.
[c]Horizontal sets of coupled signals, which may be vertically interchanged for each compound.

Table 5. ^{1}H NMR data (600 and 500 MHz, CD_3COOD-H_2O, 1:1) for amino acids in glycopeptides **5**, **7** and **9**. δ-Values in ppm

	N^xH	H^α	H^β	H^γ	H^δ	H^ε	AcHN	$N^\varepsilon H$ or NH_2
5								
Ser[a]-1	8.19	4.67	3.95/3.79	—	—	—	2.06	—
Ser[a]-2	8.33	4.69	3.97/3.80	—	—	—	—	—
Lys-3	8.31	4.47	1.89/1.77	1.48	1.72	3.06	—	7.47
Gly-4	8.08	4.27/4.05	—	—	—	—	—	—
Hyp[a]-5	—	4.54	2.52/2.15	4.60	3.81/3.76	—	—	7.70/7.02
cis-5[b]	—	4.70	2.67/2.32	4.50	–/3.61	—	—	7.87/7.22
7								
Ser[a]-1	8.19	4.68	3.97/3.83	—	—	—	2.08	—
Gly-2	8.37	4.10/4.06	—	—	—	—	—	—
Thr[a]-3	8.07	4.55	4.29	1.27	—	—	—	—
Lys-4	8.13	4.47	1.88/1.79	1.47	1.72	3.04	—	7.47
Ser[a]-5	8.30	4.65	3.97/3.79	—	—	—	—	7.68/7.14
9								
Lys-1	8.11	4.36	1.85/1.73	1.47/1.44	1.71	3.03	2.06	7.49
Gly-2	8.30	4.03/4.02	—	—	—	—	—	—
Ser[a]-3	8.19	4.74	3.97/3.80	—	—	—	—	—
Ser[a]-4	8.36	4.75	3.99/3.81	—	—	—	—	—
Ser[a]-5	8.40	4.67	3.96/3.81	—	—	—	—	7.62/7.19

[a] Denotes side chain glycosylation with Man(1→2)Man.
[b] *Cis–trans* ratio of 15:85.

C-18 column (15 μm, 300 Å, 47 mm × 300 mm) with a flow rate of 20 mL min^{-1}, and detection at 215 nm with a photodiode array detector (Waters M 991). Solvent system A: 0.1% TFA; B: 0.1% TFA in 90% acetonitrile–10% water. Gel filtration were performed on Sephadex G-10 (Pharmacia) with a flow rate of 1 mL min^{-1} and detection at 215 nm.

Definitions for MD calculations

The torsion angles φ, ψ angles for the α(1→2)-, α(1→3)- and β(1→4)-linkages (exemplified by the 1→3 case) and the φ, ψ and ω angles for the α(1→6)-linkage are defined as depicted in Scheme 2.

Initial conformations

The disaccharide residues were constructed using the builder module of InsightII (version 2.3.0, from Biosym). The 2-acetamido group of the GlcNAc was placed with the amide bond in a *trans* conformation. Initial torsion angles around the interglycosidic bonds were taken as average literature values[39–42,45,46] and from previous minimization studies[43,44] of disaccharides, (φ, ψ): (−45°, −20°) for α(1→2)-, (−50°, −20°) for α(1→3)- and (55°, 0°) for β(1→4)-linkages. For both α(1→6)-linkages, (φ, ψ) = (−60°, 180°) were employed while ω of the oxymethyl groups was allowed to attain values of both −60° and +60°, since a previous study[41]

Table 6. ^{1}H NMR data (600 and 500 MHz, CD_3COOD-H_2O, 1:1) for amino acids in glycopeptides **11** and **13**. δ-Values in ppm

	N^xH	H^α	H^β	H^γ	H^δ	H^ε	AcHN	$N^\varepsilon H$ or NH_2
11								
Thr[a]-1	8.01	4.53	4.22	1.27	—	—	2.11	—
Ala-2	8.12	4.70	1.38	—	—	—	—	—
Hyp[a]-3	—	4.63	2.53/2.12	4.61	4.06/3.81	—	—	—
cis-3[b]	—	—	2.66/2.32	—	—	—	—	—
Lys-4	8.31	4.39	1.87/1.79	1.50	1.73	3.06	—	7.48
cis-4[b]	8.54	4.37	—	—	—	—	—	—
Gly-5	8.20	4.04/4.00	—	—	—	—	—	—
Ser[a]-6	8.18	4.64	3.95/3.84	—	—	—	—	7.67/7.17
13								
Thr[a]-1	8.05	4.49	4.29	1.27	—	—	2.10	—
Ala-2	8.12	4.53	1.43	—	—	—	—	—
Gly-3	8.03	4.20/4.10	—	—	—	—	—	—
Hyp[a]-4	—	4.59	2.52/2.18	4.61	3.80/3.66	—	—	—
cis-4[c]	—	4.78	2.68/2.36	—	—	—	—	—
Gly-5	8.50	4.02/3.97	—	—	—	—	—	—
Lys-6	8.05	4.46	1.87/1.75	1.41	1.68	3.02	—	7.47
Ser[a]-7	8.21	4.66	3.97/3.82	—	—	—	—	7.62/7.16

[a] Denotes side chain glycosylation with Man(1→2)Man.
[b] Less than 2% *cis*-Hyp isomer.
[c] *Cis–trans* ratio of 10:90.

Table 7. ^1H NMR data (600 and 500 MHz, CD_3COOD-H_2O, 1:1) for amino acids in peptides **14**–**17**. δ-Values in ppm

	$N^{\alpha}H$	H^{α}	H^{β}	H^{γ}	H^{δ}	H^{ε}	AcHN	$N^{\varepsilon}H$ or NH_2
14								
Ser-1	8.10	4.52	3.88	—	—	—	2.06	—
Ser-2	8.27	4.51	3.90	—	—	—	—	—
Lys-3	8.17	4.45	1.88/1.76	1.47	1.70	3.02	—	7.44
Gly-4	8.04	4.10	—	—	—	—	—	—
Hyp-5	—	4.52	2.37/2.09	4.59	3.79/3.61		—	7.67/6.98
cis-5[a]	—	4.68	2.52/2.26	—	-/3.59	—	—	7.85/7.18
15								
Ser-1	8.19	4.47	3.94/3.86	—	—	—	2.08	—
Gly-2	8.41	4.08/4.02	—	—	—	—	—	—
Thr-3	7.97	4.40	4.27	1.20	—	—	—	—
Lys-4	8.19	4.45	1.91/1.79	1.48/1.45	1.71	3.03	—	7.47
Ser-5	8.07	4.48	3.96/3.90	—	—	—	—	7.50/7.08
16								
Thr-1	7.93	4.40	4.24	1.19	—	—	2.09	—
Ala-2	8.11	4.64	1.35	—	—	—	—	—
Hyp-3[b]	—	4.61	2.36/2.04	4.62	3.89/3.79	—	—	—
Lys-4	8.36	4.37	1.88/1.80	1.56/1.46	1.73	3.06	—	7.48
Gly-5	8.28	4.06/4.00	—	—	—	—	—	—
Ser-6	8.03	4.49	3.93/3.86	—	—	—	—	7.58/7.10
17								
Thr-1	7.91	4.39	4.27	1.20	—	—	2.10	—
Ala-2	7.99	4.48	1.40	—	—	—	—	—
Gly-3	7.99	4.02/3.94	—	—	—	—	—	—
Hyp-4	—	4.59	2.35/2.12	4.62	3.80/3.64	—	—	—
cis-4[c]	—	4.74	2.52/2.28	—	-/3.60	—	—	—
Gly-5	8.46	4.13–4.10	—	—	—	—	—	—
Lys-6	8.09	4.47	1.89/1.76	1.42	1.68	3.02	—	7.47
Ser-7	8.08	4.49	3.91/3.88	—	—	—	—	7.46/7.04

[a] *Cis–trans* ratio of 15:85.
[b] Less than 1% *cis* isomer.
[c] *Cis–trans* ratio of 10:90.

Table 8. ^1H NMR data (600 and 500 MHz, CD_3COOD–H_2O, 1:1) for dimannosyl units in glycopeptides **5**, **7** and **9**. δ-Values in ppm

		1-H	2-H	3-H	4-H	5-H	6-H
5							
Ser-1	Man(1→2)	5.03	4.11	3.87	3.97[a]	3.81–3.77	3.95–3.89/3.80–3.76
	Man(1→Ser)	5.13	3.96	3.94–3.91	3.75–3.68[b]	3.64[b]	3.95–3.89/3.80–3.76[b]
Ser-2	Man(1→2)	5.03	4.11	3.87	3.80[a]	3.81–3.77	3.95–3.89/3.80–3.76
	Man(1→Ser)	5.13	3.96	3.94–3.91	3.72[b]	3.57[b]	3.88/3.77[b]
Hyp-5	Man(1→2)	5.03	4.11	3.87	3.75–3.68[a]	3.81–3.77	3.95–3.89/3.80–3.76
	Man(1→Hyp)	5.26	3.94	3.94–3.91	3.71[b]	3.54[b]	3.88/3.76[b]
7							
Ser-1	Man(1→2)	5.03	4.08	3.86	3.97[a]	3.84–3.78	3.99–3.88/3.80–3.77
	Man(1→Ser)	5.13	3.94	3.93–3.92	3.84–3.70[b]	3.84–3.78[b]	3.99–3.88/3.80–3.77[b]
Thr-3	Man(1→2)	5.01	4.09[c]	3.86	3.84–3.70[a]	3.84–3.78	3.99–3.88/3.80–3.77
	Man(1→Thr)	5.17	3.82	3.93–3.92	3.84–3.70[b]	3.71[b]	3.99–3.88/3.80–3.77[b]
Ser-5	Man(1→2)	5.04	4.09[c]	3.86	3.84–3.70[a]	3.84–3.78	3.99–3.88/3.80–3.77
	Man(1→Ser)	5.14	3.94	3.93–3.92	3.73[b]	3.57[b]	3.88/3.78[b]
9							
Ser-3	Man(1→2)	5.05	4.10	3.87	3.97[a]	3.80–3.78	3.92/3.76
	Man(1→Ser)	5.15[b]	3.98[b]	3.94–3.91	3.74[d]	3.60[d]	3.89/3.78[d]
Ser-4	Man(1→2)	5.05	4.10	3.87	3.81[a]	3.80–3.78	3.92/3.76
	Man(1→Ser)	5.16[b]	3.96[b]	3.94–3.91	3.73[d]	3.57[d]	3.89/3.77[d]
Ser-5	Man(1→2)	5.05	4.10	3.87	3.68[a]	3.80–3.78	3.92/3.76
	Man(1→Ser)	5.15[b]	3.94[b]	3.94–3.91	3.68[d]	3.80–3.78[d]	3.92/3.76[d]

[a] Signals may be interchanged vertically for each compound.
[b,d] Horizontal sets of coupled signals, which may be interchanged vertically for each compound.
[c] Two distinct very close signals.

Table 9. ^{1}H NMR data (600 and 500 MHz, CD_3COOD–H_2O, 1:1) for dimannosyl units in glycopeptides **11** and **13**. δ-Values in ppm

		1-H	2-H	3-H	4-H	5-H	6-H
11							
Thr-1	Man(1→2)	4.98	4.10[a]	3.85	3.97[b]	3.82	3.93–3.75/3.88–3.78
	Man(1→Thr)	5.20	3.79	3.93	3.75[a,d]	3.66[d]	3.93/3.80[d]
Hyp-3	Man(1→2)	5.07	4.11	3.87	3.85[b]	3.85	3.93–3.75/3.88–3.78
	Man(1→Hyp)	5.29	3.95[c]	3.93	3.77–3.67[d]	3.71[d]	3.93–3.75/3.88–3.78[d]
Ser-6	Man(1→2)	5.03	4.10[a]	3.86	3.77–3.67[b]	3.79	3.93–3.75/3.88–3.78
	Man(1→Ser)	5.14	3.95[c]	3.93	3.75[a,d]	3.59[d]	3.88/3.78[d]
13							
Thr-1	Man(1→2)	4.98	4.09	3.86	3.99[c]	3.84–3.67	3.94–3.88/3.80–3.75
	Man(1→Thr)	5.16	3.82	3.95–3.92	3.83–3.67	3.84–3.67	3.94–3.88/3.80–3.75
Hyp-4	Man(1→2)	5.03	4.10	3.87	3.83–3.67[c]	3.76	3.94–3.88/3.80–3.75
	Man(1→Hyp)	5.28	3.94	3.95–3.92	3.83–3.67	3.84–3.67	3.94–3.88/3.80–3.75
Ser-7	Man(1→2)	5.03	4.10	3.87	3.83–3.67[c]	3.58	3.94–3.88/3.80–3.75
	Man(1→Ser)	5.14	3.96	3.95–3.92	3.83–3.67	3.84–3.67	3.94–3.88/3.80–3.75

[a,c] Two distinct very close signals.
[b,c] Signals may be interchanged vertically.
[d] Horizontal sets of coupled signals, which may be vertically interchanged for each compound.

indicated these values to be present in the four major stable conformations of mammalian $Man_9GlcNAc_2$.

Calculation procedures

All the calculations were performed using Discover (version 2.9.5) from Biosym (San Diego, California) on an Indigo 2 workstation from Silicon Graphics. The total potential energy of the molecule was calculated by adding the contributions from bond stretching, bond angle bending, torsional strain, van der Waals and electrostatic components in the Discover/Amber force field[51] (from Biosym). A distance-dependent dielectric constant of 4.0 r, which weighs the short-range interactions more than the long-range interactions, was used while calculating the electrostatic interactions. The calculations were performed in vacuo while the temperature was in the range 300–500 K. When performing the minimizations on the above four initial $Man_9GlcNAc_2$ conformations, the steepest descend algorithm was used for the first 100 steps in the energy minimization; then the conjugate minimization algorithm was used with the maximum derivative being <0.05 kcal Å^{-1} as the termination criterion.

More than 50 different tri- to octapeptide templates with three Man(1→2)Man disaccharides (ϕ, ψ = −50°, −20°) attached (X^1 arbitrarily set to 180°, 60° or −60°) were subjected to MD calculations as follows. Selected distance constraints corresponding to one of the four $Man_9GlcNAc_2$ conformations, calculated above, were set for O3 (or O4) and C1 in the two triangles formed by the terminal Man residues and the inner Man residues, respectively. Typically, the distances were constrained to within 1–2 Å using a penalty force of 5 kcal mol^{-1} Å^{-2} (allowing all the Man residues to maintain a chair conformation). After an initial minimization of 100 steps (as above), 10,000 steps (of 1

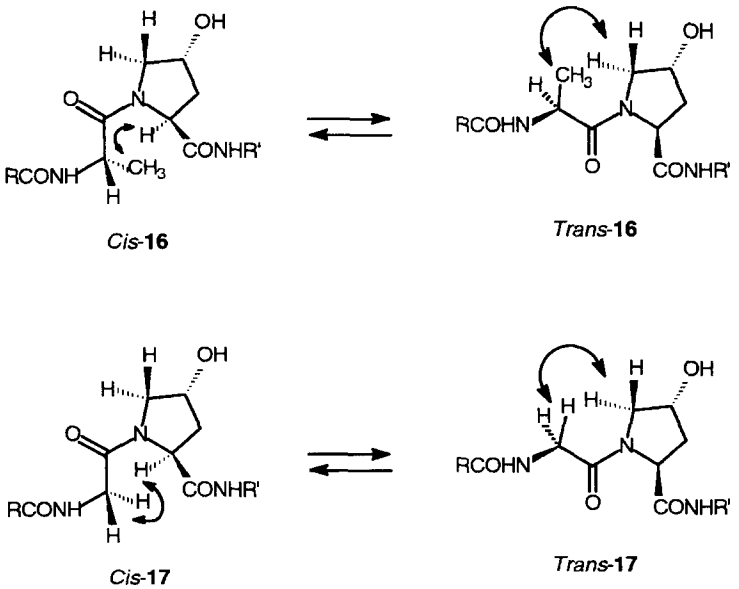

Scheme 8. Partial structures of peptides **16** and **17** showing the possible NOEs in the *cis–trans* isomers.

Table 10. ^1H NMR data (600 and 500 MHz, D_2O) for selected amino acids in peptides **14**, **16** and **17**. δ-Values in ppm

	H^α	H^β	H^γ	H^δ
14				
Hyp-5	4.48	2.33/2.07	4.59	3.76/3.61
cis-5[a]	4.67	2.49/2.25	4.51	3.73/3.56
16				
Ala-2	4.60	1.32	—	—
Hyp-3[b]	4.53	2.32/1.99	4.59	3.85/3.76
cis-3[b]	4.73	2.46/2.20	4.50	3.67/3.55
17				
Gly-3	4.05/3.97	—	—	—
cis-3	3.98/3.74	—	—	—
Hyp-4	4.48	2.27/2.03	4.54	3.71/3.56
cis-4[c]	4.67	2.43/2.19	4.45	3.68/3.50

[a] *Cis–trans* ratio of 15:85.
[b] Less than 5% *cis* isomer.
[c] *Cis–trans* ratio of 10:90.

fs) of constrained dynamic simulation were run. When a satisfactory fit between the glycopeptide and one of the four major $Man_9GlcNAc_2$ conformations was obtained (comparison by superposition, see also Figs 1 and 2), the end-conformation was minimized as described above. The best mimic for each of the four structural populations of $Man_9GlcNAc_2$ was selected as a synthetic target.

MCPS. General procedure

Synthesis of protected glycopeptides **4**, **6**, **10** and **12** and reference peptides **14–17** was performed in DMF, using the PEGA 1900/130 resin[52] with a loading of 0.36 mmol g^{-1}. The resin (a 500 mg and a 100 mg portion) was allowed to swell in DMF. Then the large portion of resin was divided into the 20 wells of the manual multiple-column peptide synthesizer[53] fitted with Teflon filters, and the small resin portion was divided into only four of the wells (referred to as 50 mg-wells) used for synthesis of non-glycosylated peptides. First, the resin was washed with 20% piperidine–DMF (0.75 mL) and subsequently with DMF (7 × 0.9 mL). The resin was derivatized with the Rink-linker[54]: to a solution (6.25 mL) of the Rink-linker (243 mg, 0.45 mmol, 2.1 eqv.) and NEM (114 μL, 0.90 mmol, 4.2 eqv.) was added TBTU (141 mg, 0.44 mmol, 2.05 eqv.),

Table 11. ^{13}C NMR data (125 MHz, D_2O) for selected amino acids in peptides **14**, **16** and **17**. δ-Values in ppm

	C^α	C^β	C^γ	C^δ
14				
Hyp-5	59.7	38.1	70.5	55.2
cis-5[a]	59.1	40.5	68.7	55.5
16				
Hyp-3[b]	59.7	37.8	70.7	56.2
17				
Hyp-4	60.2	37.8	70.6	55.3
cis-4[c]	59.3	40.3	68.7	55.5

[a] *Cis–trans* ratio of 15:85.
[b] Less than 5% *cis* isomer.
[c] *Cis–trans* ratio of 10:90.

and the mixture was kept for 10 min. Then the solution was dispensed into the wells using an Eppendorf multipipette (250 μL per 25 mg resin). After 2 h, the reagents were removed by suction and the wells were washed with DMF (6 × 0.9 mL). Acetylation of uncoupled amino groups was performed with 20% Ac_2O-DMF (300 μL per 25 mg resin) for 10 min followed by washing with DMF (8 × 0.9 mL in each well). This washing procedure was repeated after each coupling/deprotection. N^α-Fmoc deprotection was then performed with 20% piperidine-DMF (0.75 mL in each well) by two successive treatments (each 10 min). Upon suction and subsequent DMF wash, the resin was ready for the sequence of couplings. Glycosylated building block **1** (18.4 mg, 0.014 mmol, 1.5 eqv.), glycosylated building block **2** (18.6 mg, 0.014 mmol, 1.5 eqv) and glycosylated building block **3** (18.7 mg, 0.014 mmol, 1.5 eqv.) in DMF (0.25 mL) was dispensed into each of the wells, containing 25 mg resin, at the appropriate time. The non-glycosylated building blocks: Fmoc-Gly-OPfp (10.4 mg per 25 mg resin, 0.023 mmol, 2.5 eqv.), Fmoc-Ala-OPfp (10.7 mg per 25 mg resin, 0.023 mmol, 2.5 eqv.), Fmoc-Lys(Boc)-OPfp (14.2 mg per 25 mg resin, 0.023 mmol, 2.5 eqv.), Fmoc-Ser(Bu^t)-OPfp (12.4 mg per 25 mg resin, 0.023 mmol, 2.5 eqv.), Fmoc-Thr(Bu^t)-OPfp (12.7 mg per 25 mg resin, 0.023 mmol, 2.5 eqv.) and Fmoc-Hyp(Bu^t)-OPfp[26] (13.0 mg per 25 mg resin, 0.023 mmol, 2.5 eqv.) were also dissolved in DMF (0.25 mL/25 mg resin) and dispensed into the wells at the appropriate time. Each glycopeptide was synthesized in four wells (4 × 25 mg resin) whereas each of the reference non-glycosylated peptides was synthesized in a single well (50 mg resin). Before each coupling, Dhbt-OH (1.5 mg per 25 mg resin, 0.009 mmol, 1.0 eqv.) in DMF (50 μL per 25 mg resin) was added to the resin giving a very distinct yellow colour of the resin. The first amino acid derivative in DMF (0.25 mL per 25 mg resin) was then added to each well, and the synthesizer shaken gently for 2 days. After DMF wash, the Fmoc group was removed and the resin was washed as described above. The synthesis cycle was repeated until the end of each peptide (except for compounds **6**/**15** which were not Fmoc deprotected and coupled in the third cycle). After each coupling except the second, the resin was acetylated and subsequently washed as described above. The coupling times were as follows: 1 day (second coupling), 3 days (third coupling), 2 days (fourth coupling) and 3 days for each of the remaining couplings. After the last N^α-Fmoc deprotection, the resin was removed from the well(s) and transferred to a syringe (2 ml) fitted with a Teflon filter. Upon suction, the resin was acetylated as described above and then washed with DMF (8 × 1 mL) and dry CH_2Cl_2 (8 × 1 mL). Upon freeze-drying overnight the (glyco-)peptides were cleaved from the linker by treatment with 95% aq. TFA (5 mL per 25 mg resin) for 2 h, followed by filtration and washing of the resin with 95% aq. TFA and 95% HOAc. The filtrates were concentrated and the residue purified by HPLC.

Deprotection of glycopeptides. General procedure. The sugar-protected glycopeptide (~10–15 mg) was

dissolved in $CHCl_3$ (0.4 mL), and MeOH (1.6 mL) and hydrazine hydrate (0.4 mL) were added. After 3–10 h the reaction mixture was purified by directly adding it to a gel filtration (Sephadex G-10, 1 mL min^{-1}) column followed by HPLC (retention time: RT).

Ac-Ser[α-D-Man(1→2)-α-D-Man]-Ser[α-D-Man(1→2)-α-D-Man]-Lys-Gly-Hyp[α-D-Man(1→2)-α-D-Man]-NH_2 (5). Purification of the crude glycopeptide (90 mg), after TFA cleavage as described above, by preparative HPLC (elution: 50% solvent B for 10 min followed by

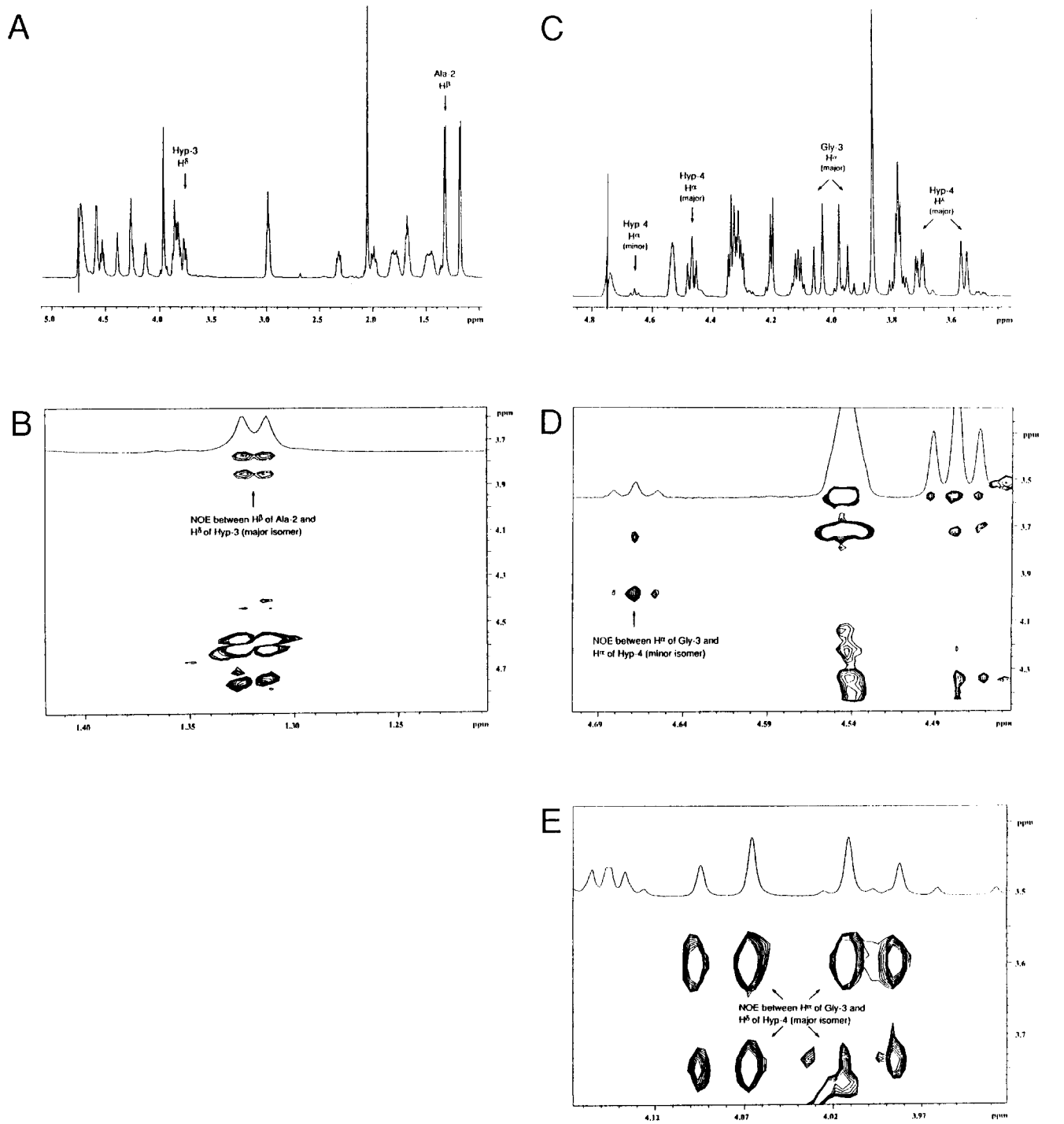

Figure 3. ^1H NMR spectra (600 MHz, D_2O) and selected NOE cross-peaks from ROESY spectra showing the assignments of *cis* and *trans* isomers of **16** and **17**. (A) Full region ^1H NMR of **16**; (B) section of the ROESY spectrum (with apartial ^1H NMR inserted) of **16**, showing the NOE between H^{β} of Ala-2 and H^{δ} of Hyp-3 in the major isomer (i.e. *trans*); (C) low field region ^1H NMR of **17**; (D) section of the ROESY spectrum (with a partial ^1H NMR inserted) of **17** showing the NOE between H^{α} of Gly-3 and H^{α} of Hyp-4 in the minor isomer (i.e. *cis*); (E) section of the ROESY spectrum (with a partial ^1H NMR inserted) of **17** showing the NOE between H^{α} of Gly-3 and H^{β} of Hyp-4 in the major isomer (i.e. *trans*).

Table 12. Human MBP ligand binding assay

Ligand	IC_{50} (mM)	Ligand	IC_{50} (mM)
Me α-D-Xyl*p*	>100	D-Man*p*	11
D-Gal*p*	>100	Me α-D-Man*p*	4
Me α-D-Gal*p*	>100	1,5-anhydromannitol	11
Me β-D-Gal*p*	>100	**5**	>2
1,5-anhydroglucitol	>100	**7**	>2
Me α-D-Glc*p*	>100	**11**	>2
Me β-D-Glc*p*	>100	**13**	>2

the linear gradients 50–80% solvent B for 40 min and 80–100% solvent B for 80 min, and then solvent B for 20 min) gave protected glycopeptide **4** (69.0 mg, 61%, RT 131.5 min). ^{1}H NMR data are presented in Tables 1 and 3. MALDI-TOF MS^+ 3133.1 $[M+H]^+$, $C_{159}H_{163}N_7O_{60}$ requires M, 3132.1.

Deacylation of compound **4** (14.1 mg) for 3 h as described in the general procedure followed by semipreparative HPLC (elution: solvent A for 30 min) gave glycopeptide **5** (5.3 mg, 78%, RT 15 min). ^{1}H NMR data are presented in Tables 5 and 8. ES-MS^+ 1505.2 $[M+H]^+$, $C_{57}H_{97}N_7O_{39}$ requires M, 1504.4.

Ac-Ser[α-D-Man(1→2)-α-D-Man]-Gly-Thr[α-D-Man-(1→2)-α-D-Man]-Lys-Ser[α-D-Man(1→2)-α-D-Man]-NH_2 (7). Purification of the crude glycopeptide (43 mg) by preparative HPLC (elution: 50% solvent B for 10 min, followed by the linear gradients 50–85% solvent B for 40 min and 85–100% solvent B for 90 min) gave protected glycopeptide **6** (26.4 mg, 23%, RT 120.5 min). ^{1}H NMR data are presented in Tables 1 and 3. MALDI-TOF MS^+ 3120.9 $[M+H]^+$, $C_{158}H_{163}N_7O_{60}$ requires M, 3120.0.

Deacylation of compound **6** (9.2 mg) for 7 h as described in the general procedure followed by semipreparative HPLC (elution: solvent A for 30 min) gave glycopeptide **7** (3.7 mg, 84%, RT 19.5 min). ^{1}H NMR data are presented in Tables 5 and 8. ES-MS^+ 1493.1 $[M+H]^+$, $C_{56}H_{97}N_7O_{39}$ requires M, 1492.4.

Ac-Lys-Gly-Ser[α-D-Man(1→2)-α-D-Man]-Ser[α-D-Man-(1→2)-α-D-Man]-Ser[α-D-Man(1→2)-α-D-Man]-NH_2(9). Protected glycopeptide **8** was synthesized in DMF by the syringe method[28] using the resin PEGA 1900/130 (loading: 0.36 mmol g^{-1}). The resin (0.48 g) was packed into a 10 mL disposable syringe fitted with a teflon filter, and connected to a suction flask through a teflon tubing with a manual 2-way teflon valve allowing excess reagent, DMF, etc., to be removed by applying vacuum. The resin was swelled in DMF and then derivatized with the Rink-linker as described in the general procedure for MCPS (including subsequent acetylation and washing). The Fmoc deprotection was performed with 20% piperidine-DMF by two successive treatments, each for 10 min. Upon suction and subsequent DMF-wash (6×5 mL), the sequential coupling of amino acids were performed. Dhbt-OH (28 mg, 0.173 mmol, 1.0 eqv.) in DMF (1 mL) and glycosylated building block **1** (282 mg, 0.207 mmol, 1.2 eqv.) in DMF (4 mL) were successively added to the resin. After a coupling time of 23 h, the resin was washed with DMF (6×5 mL) and then acetylated with 20% Ac_2O-DMF (5 mL) for 10 min. The resin was washed with DMF (8×5 mL) and Fmoc deprotected as above. The second coupling with glycosylated building block **1** (282 mg, 0.207 mmol, 1.2 eqv.) was performed for 19 h, then the resin was acetylated as above. The third coupling with glycosylated building block **1** (353 mg, 0.259 mmol, 1.5 eqv.) was performed for 21 h. The following successive couplings with Fmoc-Gly-OPfp (240 mg, 0.518 mmol, 3.0 eqv.) and Fmoc-Lys(Boc)-OPfp (273 mg, 0.432 mmol, 2.5 eqv.) were performed for 26.5 and 8 h, respectively. After the final Fmoc deprotection, the resin was washed with DMF (6×5 mL) and acetylated as above. Washing with DMF (6×5 mL) and dry CH_2Cl_2 (3×7.5 mL) was followed by freeze-drying. The protected glycopeptide was cleaved from the linker by treatment with 95% TFA (20 mL) in a flask (25 mL) for 2 h. After filtration, the resin was washed with 95% TFA, 95% HOAc and CH_2Cl_2 (each 20 mL). Concentration of the filtrates gave a crude product (96 mg) which was purified by semipreparative HPLC (elution: 50% solvent B for 10 min followed by the linear gradients 50–80% solvent B during 40 min and 80–100% solvent B during 80 min) to yield protected glycopeptide **8** (88 mg, 16%). ^{1}H NMR data are presented in Tables 1 and 3. MALDI-TOF MS^+ 3107.1 $[M+H]^+$, $C_{157}H_{161}N_7O_{60}$ requires M, 3106.0.

Deacylation of compound **8** (15.4 mg) for 10 h as described in the general procedure followed by semipreparative HPLC (elution: solvent A for 30 min) gave glycopeptide **9** (6.1 mg, 83%, RT 14.5 min). ^{1}H NMR data are presented in Tables 5 and 8. ES-MS^+ 1478.7 $[M+H]^+$, $C_{55}H_{95}N_7O_{39}$ requires M, 1478.4.

Ac-Thr[α-D-Man(1→2)-α-D-Man]-Ala-Hyp[α-D-Man-(1→2)-α-D-Man]-Lys-Gly-Ser[α-D-Man(1→2)-α-D-Man]-NH_2 (11). Purification of the crude glycopeptide (81 mg) by preparative HPLC (elution: 50% solvent B for 10 min, followed by the linear gradients 50–85% solvent B over 40 min and 85–100% solvent B over 90 min) gave protected glycopeptide **10** (62.4 mg, 54%, RT 123 min). ^{1}H NMR data are presented in Tables 2 and 4. MALDI-TOF MS^+ 3218.2 $[M+H]^+$, $C_{163}H_{170}N_8O_{61}$ requires M, 3217.2.

Deacylation of compound **10** (16.4 mg) for 10 h as described in the general procedure followed by semipreparative HPLC (elution: solvent A for 10 min followed by the linear gradient 0–25% solvent B during 50 min) gave glycopeptide **10** (7.8 mg, 96%, RT 27.5 min). ^{1}H NMR data are presented in Tables 6 and 9. ES-MS^+ 1590.1 $[M+H]^+$, $C_{61}H_{104}N_8O_{40}$ requires M, 1589.5.

Ac-Thr[α-D-Man(1→2)-α-D-Man]-Ala-Gly-Hyp[α-D-Man(1→2)-α-D-Man]-Gly-Lys-Ser[α-D-Man(1→2)-α-D-Man]-NH_2 (13). Purification of the crude glycopeptide (65 mg) by semipreparative HPLC (elution:

50% solvent B for 10 min followed by the linear gradients 50–80% solvent B during 40 min and 80–100% solvent B during 80 min) gave protected glycopeptide **12** (54.3 mg, 46%, RT 98 min). ^{1}H NMR data are presented in Tables 2 and 4. MALDI-TOF MS$^+$ 3275.5 $[M+H]^+$, $C_{165}H_{173}N_9O_{62}$ requires M, 3274.2.

Deacylation compound **12** (10.6 mg) for 10 h as described in the general procedure followed by semipreparative HPLC (elution: solvent A for 10 min followed by the linear gradient 0–30% solvent B during 60 min) gave glycopeptide **13** (2.7 mg, 51%, RT 26.5 min). ^{1}H NMR data are presented in Tables 6 and 9. ES-MS$^+$ 1647.1 $[M+H]^+$, $C_{63}H_{107}N_9O_{41}$ requires M, 1646.6.

Ac-Ser-Ser-Lys-Gly-Hyp-NH$_2$ (14). Purification of the residue from TFA cleavage by semipreparative HPLC (elution: solvent A for 30 min) gave peptide **14** (6.6 mg, 69%, RT 18.5 min). ^{1}H NMR data and selected ^{13}C NMR data are presented in Tables 7, 10 and 11, respectively. ES-MS$^+$ 532.4 $[M+H]^+$, $C_{21}H_{37}N_7O_9$ requires M, 531.6.

Ac-Ser-Gly-Thr-Lys-Ser-NH$_2$ (15). Purification of the residue from TFA cleavage by semipreparative HPLC (elution: solvent A for 30 min) gave peptide **15** (2.1 mg, 22%, RT 16.5 min). ^{1}H NMR data and selected ^{13}C NMR data are presented in Tables 7 and 11, respectively. ES-MS$^+$ 520.4 $[M+H]^+$, $C_{20}H_{37}N_7O_9$ requires M, 519.6.

Ac-Thr-Ala-Hyp-Lys-Gly-Ser-NH$_2$ (16). Purification of the residue from TFA cleavage by semipreparative HPLC (elution: solvent A for 10 min followed by the linear gradient 0–20% solvent B during 40 min) gave peptide **16** (4.8 mg, 43%, RT 7.5 min). ^{1}H NMR data and selected ^{13}C NMR data are presented in Tables 7, 10 and 11, respectively. ES-MS$^+$ 617.4 $[M+H]^+$, $C_{25}H_{44}N_8O_{10}$ requires M, 616.7.

Ac-Thr-Ala-Gly-Hyp-Gly-Lys-Ser-NH$_2$ (17). Purification of the residue from TFA cleavage by semipreparative HPLC (elution: solvent A for 30 min followed by the linear gradient 0–5% solvent B during 30 min) gave two close peaks (RT 41 min and 44 min), which showed similar $[M+1]$ peaks at m/z ~674–675. The fractions were combined and yielded peptide **17** in (4.3 mg, 35%). ^{1}H NMR data and selected ^{13}C NMR data are presented in Tables 7, 10 and 11, respectively. ES-MS$^+$ 674.4 $[M+H]^+$, $C_{27}H_{47}N_9O_{11}$ requires M, 673.7.

Analysis of the binding affinity of glycopeptides 5, 7, 11 and 13 for human MBP

The analysis was carried out as an inhibition assay using the time resolved immuno-fluorometric assay (TRIFMA) technique. Microtitre wells were coated with mannan and incubated with MBP together with each of the glycopeptides **5**, **7**, **11** and **13**, and the following monosaccharides (and some derivatives): Me α-D-Glc, Me β-D-Glc, 1,5-anhydromannitol, Gal, Me α-D-Gal, Me β-D-Gal, Me α-D-xylopyranose, Me α-D-Man, Man and 1,5-anhydromannitol.

The wells of microtitre plates (Fluoro plates, Nunc A/S, Kamstrup, Denmark) were coated with mannan (purified from *Saccharomyces cerevisiae*) by incubation with mannan (70 ng) in coating buffer (100 µL, 0.1 M $NaHCO_3$, pH 9.6) overnight at room temperature. Subsequently the wells were washed with TBS (0.15 M NaCl, 10 mM Tris–HCl, 7.5 mM NaN_3, pH 7.4), and residual binding capacity was blocked through incubation with human serum albumin (1 mg per ml TBS) for 1 h and wash with TBS–Tween (0.05% Tween 20 in TBS buffer).

To the wells were then applied TBS–Tween (100 µL, 5 mM $CaCl_2$ and with 0.1% human serum albumin added) also containing a mixture of MBP (20 ng mL^{-1}) and the relevant glycopeptides at final concentrations of 2, 0.4, 0.08 and 0.016 mM or the monosaccharides at 100, 33.3, 11 and 3.7 mM, while other derivatives were tested at 12.5, 4.1, 1.3 mM and 0.46 mM. As a control for total inhibition, MBP was added in buffer with 10 mM EDTA instead of $CaCl_2$.

The plates were incubated overnight at 4 °C and washed with TBS–Tween (5 mM $CaCl_2$). Then TBS–Tween (100 µL, 25 µM EDTA), containing monoclonal anti-MBP antibody (20 ng, MAB 131–1, The State Serum Institute, Copenhagen, Denmark) labelled with europium, was added to each well. The antibody was labelled with europium chelated to phenylisothiocyanate-diethyl-triamin-tetra acetic acid according to the manufacturers recommendations (Wallac Oy, Turku, Finland) at pH 8.5, which in preliminary trials was found optimal.

After incubation for 2 h at room temperature, the plates were washed with TBS–Tween (5 mM $CaCl_2$). Enhancement solution [0.1 M sodium acetate with potassium hydrogenphtalate to pH 3.2, also containing 15 µM 2-naphthoyltrifluoroacetone, 50 µM tri-*n*-octylphosphine oxide, 4% polyethylene glycol 6000 and 0.1% (v/v) Triton X-100] was added, and following mixing (5 min) and incubation for 10 min, fluorescence was measured on a time resolved spectrofluorometer (Delfia 1232, Wallac, Oy).

Acknowledgements

This work was supported by the EU-Science Programme (M.M. grant SCI*-CT92–0765). We thank Mr Bent. Ole Petersen for recording the 600 MHz NMR spectra, and Dr Anita Jansson-Mathiesen for recording the ES-MS spectra.

References

1. Drickamer, K. In *Molecular Biology*; Fukuda, M.; Hindsgaul, O., Eds.; Oxford University: Oxford, 1994; pp 53–87.

2. Holmskov, U.; Malhotra, R.; Sim, R.B.; Jensenius, J.C. *Immunol. Today* **1994**, *15*, 67.

3. Kawasaki, N.; Kawasaki, T.; Yamashina, I. *J. Biochem (Tokyo)* **1983**, *94*, 937.

4. Holmskov, U.; Holt, P.; Reid, K. B. M.; Willis, A.C.; Teisner, B.; Jensenius, J.C. *Glycobiology* **1993**, *3*, 147.

5. Kozutsumi, Y.; Kawasaki, T.; Yamashina, I. *Biochem. Biophys. Res. Commun.* **1980**, *95*, 658.

6. Oka, S.; Ikeda, K.; Kawasaki, T.; Yamashina, I. *Arch. Biochem. Biophys.* **1988**, *260*, 257.

7. Sastry, K.; Zahedi, K.; Lelias, J. M.; Whitehead, A. S.; Ezekowitz, R. A. *J. Immunol.* **1991**, *147*, 692.

8. Laursen, S. B.; Hedemand, J. E.; Thiel, S.; Willis, A. C.; Skriver, E.; Madsen, P. S.; Jensenius, J. C. *Glycobiology* **1995**, *5*, 553.

9. Sheriff, S.; Chang, C.-Y. Y.; Ezekowitz, R. A. B. *Nature, Struct. Biol.* **1994**, *1*,

10. Hoppe, H. J.; Reid, K. B. M. *Protein Sci.* **1994**, *3*, 1143.

11. Reid, K. B. M. *Biochem. Soc. Trans.* **1983**, *11*, 1.

12. Ikeda, K.; Sannoh, T.; Kawasaki, N.; Kawasaki, T.; Yamashina, I. *J. Biol. Chem.* **1987**, *262*, 7451.

13. Lu, J. H.; Thiel, S.; Wiedemann, H.; Timpl, R.; Reid, K. B. *J. Immunol.* **1990**, *144*, 2287.

14. Ohta, M.; Okada, M.; Yamashina, I.; Kawasaki, T. *J. Biol. Chem.* **1990**, *265*, 1980.

15. Kawasaki, N.; Kawasaki, T.; Yamashina, I. *J. Biochem.* **1989**, *106*, 483.

16. Kuhlman, M.; Joiner, K.; Ezekowitz, R. A. *J. Exp. Med.* **1989**, *169*, 1733.

17. Summerfield, J. A. *Biochem. Soc. Trans.* **1993**, *21*, 473.

18. Sathyamoorthy, N.; Decker, J. M.; Sherblom, A. P.; Muchmore, A. *Molec. Cellu. Biochem.* **1991**, *102*, 139.

19. Basse, C. W.; Bock, K.; Boller, T. *J. Biol. Chem.* **1992**, *267*, 10258.

20. Voyer, N.; Lamothe, J. *Tetrahedron* **1995**, *51*, 9241.

21. Lavielle, S.; Ling, N.C.; Guillemin, R.C. *Carbohydr. Res.* **1981**, *89*, 221.

22. Powell, M.F.; Stewart, T.; Otvos, L.; Urge, L.; Gaeta, F.C.A.; Sett, A.; Arrhenius, T.; Thomson, D.; Soda, S.; Colon, S.M. *Pharm. Res.* **1993**, *10*, 1268.

23. Takeda, T.; Kanemitsu, T.; Ishiguro, M.; Ogihara, Y.; Matsubara, M. *Carbohydr. Res.* **1994**, *256*, 59.

24. Polt, R.; Porreca, F.; Szabo, L.Z.; Bilsky, E.J.; Davis, P.; Abbruscato, T.J.; Davis,T.P.; Horvath, R.; Yamamura, H.I.; Hruby, V.J. *Proc. Natl. Acad. Sci. USA* **1994**, *91*, 7114.

25. Rademann, J.; Schmidt, R.R. *Carbohydr. Res.* **1995**, *269*, 217.

26. Franzyk, H.; Meldal, M.; Paulsen, H.; Bock, K. *J. Chem. Soc., Perkin Trans. 1* **1995**, 2883.

27. Peters, S.; Bielfeldt, T.; Meldal, M.; Bock, K.;Paulsen, H., *J. Chem. Soc., Perkin Trans 1* **1992**, 1163.

28. Christiansen-Brams, I.; Meldal, M.; Bock, K. *J. Chem. Soc., Perkin Trans. 1* **1993**, 1461.

29. Christensen, M. K.; Meldal, M.; Bock, K.; Cordes, H.; Mouritsen, S.; Elsner, H. *J. Chem. Soc., Perkin Trans. 1* **1994**, 1299.

30. Christensen, M. K.; Meldal, M.; Bock, K. *J. Chem. Soc., Perkin Trans. 1* **1993**, 1453.

31. Lee, R. T.; Lin, P.; Lee, Y. C. *Biochemistry* **1984**, *23*, 4255.

32. Ozaki, K.; Lee, R. T.; Lee, Y. C.; Kawasaki, T. *Glycoconjugate J.* **1995**, *12*, 268.

33. Kichler, A.; Schuber, F. *Glycoconjugate J.* **1995**, *12*, 275.

34. Biessen, E. A. L.; Beuting, D. M.; Roelen, H. C. P. F.; van de Marel, G. A.; van Boom, J. H.; van Berkel, T. J. C. *J. Med. Chem.* **1995**, *38*, 1538.

35. Tong, P. Y.; Gregory, W.; Kornfeld, S. J. *J. Biol. Chem.* **1989**, *264*, 7962.

36. Iobst, S. T.; Wormald, M. R.; Weis, W. I.; Dwek, R.A.; Drickamer, K. J. *J. Biol. Chem.* **1994**, *269*, 15505.

37. Lee, R. T.; Ichikawa, Y.; Kawasaki, T.; Drickamer, K.; Lee, Y. C. *Arch. Biochem. Biophys.* **1992**, *299*, 129.

38. Nakahara, Y.; Shibayama, S.; Nakahara, Y.; Ogawa, T. *Carbohydr. Res.* **1996**, *280*, 67.

39. Homans, S. W.; Dwek, R. A.; Rademacher, T. W. *Biochemistry* **1987**, *26*, 6553.

40. Homans, S. W.; Pastore, A.; Dwek, R. A.; Rademacher, T. W. *Biochemistry* **1987**, *26*, 6649.

41. Wooten, E. W.; Bazzo, R.; Edge, C. J.; Zamze, S.; Dwek, R. A.; Rademacher, T.W. *Eur. Biophys. J.* **1990**, 18, 139.

42. Balaji, P. V.; Quasba, P. K.; Rao, V. S. R. *Glycobiology*, **1994**, *4*, 497.

43. Spronk, B. A..; Rivera-Sagredo, A.; Kamerling, J. P.; Vliegenhart, J. F. G. *Carbohydr. Res.* **1995**, *273*, 11.

44. Dowd, M. K.; French, A. D. *J. Carbohydr. Chem.* **14**, 589.

45. Paulsen, H. *Angew. Chem.* **1990**, *8*, 823.

46. Stuike-Prill, R.; Meyer, B. *Eur. J. Biochem.* **1990**, *194*, 903.

47. Schultheiss-Reimann, P.; Kunz, H. *Angew. Chem.* **1983**, *95*, 64.

48. Vliegenthart, J. F. G.; Dorland, L.; van Halbeek, H. *Adv. Carbohydr. Chem. Biochem.* **1983**, *41*, 209.

49. Garbay-Jaureguiberry, C.; Arnoux, B.; Prangé, T.; Wehri-Altenburger, S.; Pascard, C.; Roques, B. P. *J. Am. Chem. Soc.* **1980**, *102*, 1827.

50. Fan, J-Q.; Quesenberry, M.S.; Takegawa, K.; Iwahara, S.; Kondo, A.; Kato, I.; Lee, Y. C. *J. Biol. Chem.* **1995**, *270*, 17730.

51. Homans, S. W. *Biochemistry* **1990**, *29*, 9110.

52. Auzanneau, F.-I.; Meldal, M.; Bock, K. *J. Pept. Sci.* **1995**, *1*, 31.

53. Meldal, M.; Breddam, K. In *Innovation and Perspectives in Solid Phase Synthesis*; Epton, R., Ed.; SPCC: Birmingham, 1990; pp 533.

54. Rink, H. *Tetrahedron Lett.* **1987**, *28*, 3787.

(*Received in U.S.A.* 30 *January* 1996; *accepted* 17 *May* 1996)